



# Radio frequency processing and recent advances on thawing and tempering of frozen food products

Yvan Llave & Ferruh Erdogdu

To cite this article: Yvan Llave & Ferruh Erdogdu (2020): Radio frequency processing and recent advances on thawing and tempering of frozen food products, Critical Reviews in Food Science and Nutrition, DOI: [10.1080/10408398.2020.1823815](https://doi.org/10.1080/10408398.2020.1823815)

To link to this article: <https://doi.org/10.1080/10408398.2020.1823815>



Published online: 22 Sep 2020.



Submit your article to this journal [↗](#)



Article views: 9



View related articles [↗](#)



View Crossmark data [↗](#)

REVIEW



# Radio frequency processing and recent advances on thawing and tempering of frozen food products

Yvan Llave<sup>a</sup>  and Ferruh Erdogdu<sup>b</sup> 

<sup>a</sup>Department of Agro-Food Science, Niigata Agro-Food University, Niigata, Japan; <sup>b</sup>Department of Food Engineering, Ankara University, Ankara, Turkey

## ABSTRACT

During radio frequency (RF) thawing—tempering (defrosting) of frozen food products, some regions, mostly along the corners and edges, heat—thaw first due to the strong interaction of electric field and evolved heating leading to temperature increase. Resulting higher power absorption along these regions, compared to the rest of the volume, is the major cause of this problem. Besides, increase in temperature with phase change results in a significant increase of dielectric properties. This situation leads to runaway heating, which triggers the non-uniform temperature distribution in an accelerated manner. All these power absorption and temperature non-uniformity-based changes lead to significant quality changes, drip losses, and microbial growth. Based on this background, the objective of this review was to provide a comprehensive background regarding the most relevant and novel defrosting application studies using RF process, dielectric property data for frozen foods in the RF band, and novel mathematical modeling based computer simulation approaches to achieve a uniform process. Experimental and modeling studies were related with electrode position, sample geometry and size, electrode gap of the applied RF process, and the potential of charged electrode. Applying translational and rotational movement of the food product and the charged electrode vertical movement during the process to adjust the electric field and use of two-cavity systems and curved electrodes were also explained in detail. The data presented in this review is expected to give an insight information for further development of innovative RF thawing/tempering systems.

## KEYWORDS

Computer simulation; defrosting; dielectric properties; frozen foods; mathematical modeling; radio frequency

## Introduction

Shelf life of refrigerated food products, mainly meat, fish, and seafood, is limited because of the microbial growth and enzymatic activities. Therefore, freezing is an effective process and widely applied preservation method to ensure safety and quality retention of these food products until their utilization specifically in further industrial processes (Boonsumrej et al. 2007) or immediate consumption upon thawing. In meat (beef, pork, and poultry) and seafood processing industries, freezing based preservation methods are highly applicable and have been widely used for a long time. However, frozen products, as indicated, need to be tempered or thawed to a reasonable temperature for further processing or size reduction for the purpose of a further process (Taher and Farid 2001). Defrosting of frozen food products is also a fundamental process at household conditions (home and restaurant). The US Food and Drug Administration (FDA) recommends thawing methods in a refrigerated temperature ( $\leq 5^{\circ}\text{C}$ ), or completely submerging the frozen food under running water at  $21^{\circ}\text{C}$  or below (FDA Food Code 2013). Some of the most relevant industrial thawing/tempering applications include

- Tempering meat from frozen state to a transition phase ( $-5 \sim 0^{\circ}\text{C}$ ) allowing it to become more malleable and easier to handle for further mechanical operations (e.g., size reduction) (Zhu et al. 2019),
- Use/cooking of frozen perishable foods transported and stored over a long period of time (e.g., military rations) (Karthikeyan et al. 2015),
- Tempering frozen pork blocks before processing such as slicing, tenderizing, breading, and frying (Choi et al. 2017),
- Tempering of frozen minced fish (blocks) before being further processed or chopped into surimi (Yang et al. 2019), and
- Tempering of frozen surimi blocks to prepare surimi-based products such as kamaboko, fish balls, and others.

Inappropriate selection of the thawing/tempering method would result in food quality degradation, especially changes in texture, flavor, color, lipid, and protein oxidations in addition to the possible microbial growth and spoilage (Jia et al. 2017). Therefore, the main goal of an optimal thawing/tempering process in an industrial setting is to minimize process

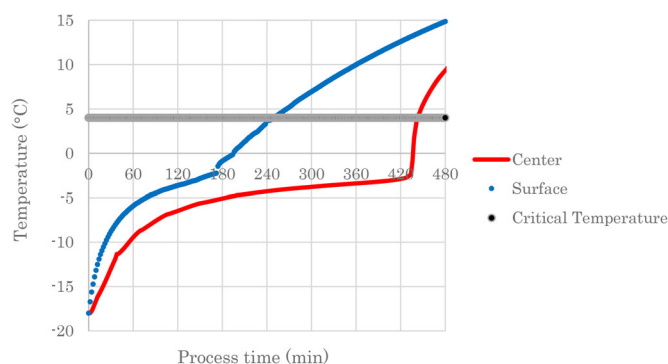


**Figure 1.** Center and surface temperature change of a large-sized frozen meat block during a conventional air thawing process. [From Singh, Erdogan, and Mannapperuma (2002)].

time while limiting quality losses and microbial growth (Bedane et al. 2018).

Conventional thawing approaches use air or water for heat transfer by convection onto the surface of the food product. The heat on the surface is then conducted through the inside of the product while the thawed surface with a lower thermal conductivity acts as an insulator to the product surrounded by this layer. As the product keeps thawing, thickness of the insulating layer increases, making the thawing process slow and requiring longer time depending on the size and shape of the food product. A lengthy thawing process promotes significant drip losses, microbial growth, and quality degradation. (Jiao et al. 2018). These changes in quality parameters are rather significant aspects in food industry both in consumer and financial point of view (Gambuteanu and Alexe 2015). Higher temperatures (over  $+4^{\circ}\text{C}$ ) are mostly observed over the product surface (higher temperature medium of water or air is preferred to shorten the thawing time in the conventional approaches), and this leads to possible microbial growth with quality losses. Figure 1 demonstrates the change in the center and surface temperatures of a larger sized food product (to represent a  $\approx 6$  kg block of meat in the dimensions of  $0.16 \times 0.18 \times 0.20$  m) experiencing a conventional air thawing process (Singh, Erdogan, and Mannapperuma 2002). The applied air medium was at temperature of  $20^{\circ}\text{C}$  and under natural convection thawing conditions.

In general, defrosting process is applied to thaw (temperature being just above the product's freezing point  $\approx$  to  $0^{\circ}\text{C}$  at the thermal center) or temper (temperature being just below the product's freezing point  $\approx$  to  $-5 \sim -2^{\circ}\text{C}$  at thermal center) depending upon the target final temperature. Compared to the conventional thawing approaches, so-called proper thawing procedures, tempering approaches can be carried out in shorter processing times, reduce the quality loss, and do not allow microbial growth keeping the food product at a desired safety.

In recent years, several new thawing technologies have been extensively studied. These were rather rapid thawing approaches compared to the conventional cases, and they were reported to avoid problems related to longer thawing times and changes in quality attributes. Thermal processes such as dielectric (microwave—MW and radio frequency—

RF) or resistive heating have the benefit of being rapid and convenient while further challenges of these processes include runaway heating leading to surface over-heating especially along the corner and edges and high energy consumption (Cai et al. 2019). Non-thermal processes such as ultra-high pressure (Rouille et al. 2002; Zhu, Su et al. 2014), ultrasound (Li et al. 2020; Wang et al. 2020) and vacuum thawing (Cai et al. 2018; Wang et al. 2020) have been applied in the last few decades and also known to reduce food losses in quality. These approaches are still not observed to be feasible and adapt to industrial processes especially for larger sized products. Among the dielectric heating methods, MW applications are rather attractive in the literature to promote a quick thawing—tempering method, but limited wavelength and resulting penetration depth specifically at the frozen conditions ( $<0^{\circ}\text{C}$ ) limits this approach for an effective industrial process specifically for larger sized products. The unrequired surface heating and thermal runaway are the unavoidable consequences.

Recently, thawing of frozen blocks of meat and seafood by RF has been commercially applied [SAIREM SAS (France); SONAR (Turkey); Stalam (Italy); Yamamoto Vinita (Japan)] with several advantages over conventional thawing methods and MW applications. These advantages include reduced thawing time and less damage to product quality owing to the volumetric heating characteristic with the longer penetration depth. RF process provides the ability to penetrate deep (due to the longer wavelength, e.g.,  $\approx 11$  m at  $27.12$  MHz frequency) and possibilities to heat food products even within the package itself. In addition, drip losses were minimized with the reduced process time, and microbial safety was not compromised (Li and Sun 2002).

Energy consumption in the food industry has been the focus especially for the last two years, and the increasing demand for the food safety. This led to a higher consumption of hot and cold water in the increased cleaning cycles (Pereira and Vicente 2010). Innovative approaches like the RF use in food processing can provide energy savings with the reduced process times and water savings. Considering the focus of current review, water usage for thawing purposes is common application in the industry with certain impacts on the energy and environment. The first thing to carry out with the water used in a thawing process is pre-treatment for refining before releasing to the environment. The opposite case causes environmental pollution-based problems while the water demand is an additional energy spending for the given industry.

Considering that the traditional—conventional processes depend upon the time—temperature change of the product with the requirement of large water consumption and also fossil consumption (Pereira and Vicente 2010), introduction of innovative RF process might lead to a certain savings on this front with additional benefits for the environmental aspects. However, it should be noted that the economics of this innovative process needs a careful assessment in the view of capital cost (Maloney and Harrison 2016). In addition, the economical constraint of RF (more expensive than the conventional processes in the view of power output)

**Table 1.** Comparison of major characteristics between radio frequency (RF) and microwave (MW) frequencies more used in the food industry.

	RF			MW	
ISM frequencies (MHz)	13.56	27.12	40.68	915	2450
Wavelength in vacuum (m)	22.1	11.1	7.4	0.33	0.12
Penetration depths in tap water (m)	1.58	0.79	0.53	0.02	0.01
Major heating mechanism	Ionic charge migration			Dipole water molecule agitation	
System construction	Simple			Complicated	

Adapted from Jiao et al. (2018).

(Swamy and Muthukumarappan 2021) is the certain limit for preferring of these systems by the SMEs while this process provides a certain quality with reduced environmental cost and increased energy saving as stated above.

Within the last ten years or so, although the literature of RF thawing/tempering studies have increased, it is also evident that more research is required to make RF technology more applicable for an industrial process. A number of problems remain to be addressed due to non-uniformity of temperature distribution within the food product, and possible ways to mitigate higher temperatures encountered over the surfaces and edges—corners of the product. In this review, recent literature on RF thawing and tempering of frozen products, with experimental and mathematical modeling approaches to improve heating uniformity, has been summarized with the aim to help innovate the RF process for an industrial application.

Based on the given background of the industrial defrosting of frozen food products, the objectives of this review are:

- to introduce the basic principles of RF process,
- to present an overview of recent developments in the RF thawing/tempering of frozen foods,
- to introduce and analyze the recent published mathematical modeling studies for simulation of RF thawing/tempering to assist improving the temperature uniformity and avoid runaway heating, and
- to propose recommendations for future research to enhance practical applications in the thawing/tempering of frozen food industry.

## Radio frequency heating basics

### Principles of radio frequency heating

In a simple definition, RF process is based on the capacitor (to store the electromagnetic energy in an electromagnetic field) principle in the physics point of view. In an RF cavity, there are two electrodes placed where one of them is set up to be the ground to store the energy while the other one is the potential applied electrode. The product is placed between these two electrodes and during the process the electromagnetic energy is absorbed. It is converted to the heat energy through bipolar rotation and ionic conduction mechanism where the latter one is more effective in an RF process compared to the MW applications. This interaction mechanism is explained below in detail.

RF, like MW application with shorter wavelength, is a non-ionizing form of electromagnetic energy (Mitchell

2016). Electromagnetic waves at specific frequencies were allocated for industrial, scientific, and medical (ISM) uses by the US Federal Communication Commission (FCC): 13.56, 27.12, and 40.68 MHz for RF and 915, 2,450, and 5,800 MHz besides 24,124 GHz for MW, respectively. Besides the lower frequency and significant penetration depth, RF (in the frequency range from 300 kHz to 300 MHz) heating provides a quick heat generation within the food matrices interacting with ions, atoms, and molecules to generate the internal heat (Jiao, Luan, and Tang 2014). The higher frequency of MW application results in higher power absorption and heat energy generation inside the food product while the penetration depth is limited compared to the RF application. Penetration depth is therefore a significant property to lead to the heat generation inside the product. It is a function of dielectric properties (DPs) and depends upon the applied frequency. For food products, a general comment is that at lower frequencies, the energy might reach deeper into the food product compared to higher frequency applications. This is due to the wavelength and makes the RF method more suitable for large-scale industrial applications with its applied frequency of 13.56 and 27.12 MHz, the most preferred frequencies (Wang et al. 2003). Llave et al. (2014) reported penetration depths in the range of 0.15 to 4.2 m and 0.09 to 2.3 m for the same tuna sample at 13.56 and 27.12 MHz, respectively in a defrosting process  $-20$  to  $10^{\circ}\text{C}$ . With these controversial properties, RF has an easier way of controlling during a process in the view of temperature increase and a better temperature uniformity due to its penetration depth. Again, this makes the RF application more suitable for processing bulk products (Guo, Mujumdar, and Zhang 2019). The wavelength of electromagnetic waves at some specific frequencies and the penetration depth in tap water at room temperature for MW and RF are shown in Table 1.

In traditional RF heating, such as in parallel plate electrode systems, the electromagnetic field is usually generated in a directional way between the electrode plates (Figure 2), while the electromagnetic field of MW heating might approach the material from different directions based on the various cavity design, magnetron structure, and location of the waveguides (Huang et al. 2016). Consequently, compared to the complex and non-uniform field in MW cavities, RF heating usually offers a simpler and comparatively more uniform electromagnetic field even though the resulting uniformity is still a major concern of the literature and the industrial processes. As demonstrated in Figure 2, the electric field, generated over the charged electrode (top electrode in Figure 2), moves toward the ground electrode and absorbed by the product placed between. With this

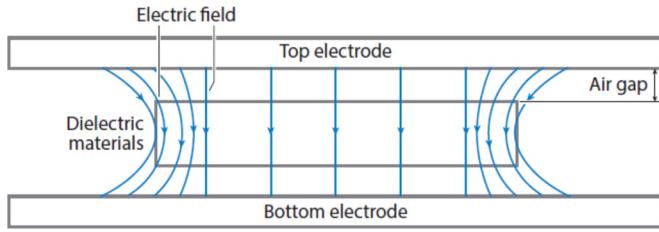


**Figure 2.** The electric field strength between two parallel plate electrodes with a dielectric sample slab placed in the center and middle in a RF heater cavity showing fringing field at the sample edges. [From Huang et al. (2016) with permission from Elsevier].

conventional design, fringing of the electric field through the corners is also observed. This behavior over the corners was defined as magnet-like effect by Erdogan et al. (2017). The magnet-like effect among the product edges—corners and the electric field is significantly observed during a continuous process.

A successful dielectric heating process is carried out where there is polarization by an electric field (e.g., foods containing plus and minus charged ions such as those present in water molecules and in the protein structure). In an oscillating electric field, the molecules start rotating and colliding with other molecules, and the increase in the kinetic energy leads to heat generation. Besides the ionic movement, when food materials are treated with RF, polar molecules start dipole rotation with the alternating electromagnetic field. This also helps converting the electromagnetic energy into heat energy, especially in the frozen products. This specifically starts with the phase change along the surface, edges, and corners. The thawing process is then accelerated due to the increase in the DPs (phase change from ice to water leads to a certain jump in the DPs where the absorption of the electromagnetic energy and conversion to heat is increased). While the polarization demonstrates its effect, the dissociated ions start moving again with the alternating electrical field and generate heat by the friction among molecules (Jiao, Luan, and Tang 2014).

### Dielectric properties of frozen foods

For dielectric heating applications, DPs are the most important physical properties governing the penetration depth, electromagnetic field distribution within the product, and the power absorption by conversion of electromagnetic energy into heat energy (Jiao, Tang et al. 2014). DPs are the intrinsic properties describing the degree of a material's interaction with an alternative electrical field, and quantifying its ability for reflecting, storing, and transmitting the electromagnetic energy (Datta, Sumnu, and Raghavan 2014). The DPs are expressed by Eq. (1) (Datta, Sumnu, and Raghavan 2014):

$$\epsilon_r^* = \epsilon_r' - j\epsilon_r'' \quad (1)$$

where  $\epsilon_r^*$  is the complex relative (to vacuum) permittivity;  $\epsilon_r'$  is the relative dielectric constant (ability of the material to absorb the electromagnetic energy;  $j$  is the imaginary unit ( $\sqrt{-1}$ ); and  $\epsilon_r''$  is the relative dielectric loss factor (measure of

the ability of a material to dissipate electromagnetic energy into heat energy). It should be indicated that the dielectric constant and dielectric loss factor are dimensionless quantities, and they are defined relative to the permittivity of the space (Datta, Sumnu, and Raghavan 2014).

Considering the requirement of solving the Maxwell's equations to determine the electromagnetic field energy distribution inside the RF cavity, knowledge of the DPs as a function of temperature is required. The differential form of Maxwell's equations are as follows (Knoerzer, Regier, and Schubert 2008):

$$\nabla \cdot \vec{B} = \nabla \cdot \mu \vec{H} = 0 \quad (2)$$

$$\nabla \cdot \vec{D} = \nabla \cdot \epsilon_r \vec{E} = \rho_m \quad (3)$$

$$\nabla \times \vec{H} = \frac{\partial \vec{D}}{\partial t} + J = \frac{\partial \epsilon_r \vec{E}}{\partial t} + \sigma \vec{E} \quad (4)$$

$$\nabla \times \vec{E} = -\frac{\partial \vec{B}}{\partial t} = -\frac{\partial \mu \vec{H}}{\partial t} \quad (5)$$

$$\sigma = \epsilon_0 \epsilon_r'' \omega \quad (6)$$

where  $\vec{E}$  is the electric-field intensity ( $\text{V m}^{-1}$ );  $\vec{H}$  is the magnetic-field intensity ( $\text{A m}^{-1}$ );  $\vec{B}$  is the magnetic induction ( $\text{Wb m}^{-2}$ );  $\vec{D}$  is the electric displacement ( $\text{C m}^{-2}$ );  $\rho_m$  is the electric volume charge density ( $\text{C m}^{-3}$ );  $J$  is the current flux ( $\text{A m}^{-2}$ );  $\epsilon_r$  is the complex permittivity (Eq. 3); and permeability  $\mu$  can be expressed using the magnetic permeability of free space:  $\mu_0 = 4\pi \times 10^{-7}$  ( $\text{H m}^{-1}$ ). Electric conductivity  $\sigma$  ( $\text{S m}^{-1}$ ) is related to the relative dielectric loss factor of the material,  $\omega$  ( $= 2\pi f$ , where  $f$  is the frequency of the RF wave) is the angular frequency ( $\text{rad s}^{-1}$ ), and  $\epsilon_0 = 8.854 \times 10^{-12}$  ( $\text{F m}^{-1}$ ) is the permittivity of free space.

In Table 2, some of the most relevant published DPs data of several frozen foods at specified frequencies are summarized. Different kinds of frozen food materials might have diverse DPs. Even in the same food product, the DPs of different sections might be discrepant. For example, Llave et al. (2014) reported that different sections of the same tuna body had differences in their DPs (see Table 2), basically due to difference in their chemical composition. From Table 2, it can also be observed that most of the reported data was at the popular frequency of 27.12 MHz and that the dielectric constant and dielectric loss factor values increased with temperature. It should also be indicated that it is not possible to expect a trend in the variation of the DPs among the food products, since not only temperature but also applied frequency and composition are the major contributors to their variation (Farag et al. 2011; Llave et al. 2014; Piyasena et al. 2003; Zhang, Lyng, and Brunton 2004). In addition, it should be emphasized that the food engineering literature currently lacks in the DPs data in the RF frequencies within the frozen range. More details of the effect of frequency, temperature, and composition on the DPs of frozen foods, at the RF range, can be found in previous published works in this field (Awuah, Ramaswamy, and Tang 2014; Llave and Sakai 2018).



**Table 2.** Dielectric properties of selected frozen foods in the radio frequency range.

Frozen foods	Frequency (MHz)	Temperature (°C)	$\epsilon'_r$	$\epsilon''_r$	References
Beef blends (lean:67.8 % and 11.8 % of moisture and fat content, respectively)	27.12	−15	22.3	28.8	Farag et al. (2008)
		−5	36	81.4	
		−3	51.2	149.3	
		−1	68.8	241.9	
Beef blends (50:50, lean:fat; 48.2 % and 36.1 % of moisture and fat content, respectively)	27.12	−15	18.4	23.4	Farag et al. (2008)
		−1	37.3	92.4	
		−15	9.7	7.7	
		−1	18.3	26.1	
Beef blends (full fat; 26.3 % and 65.7 % of moisture and fat content, respectively)	27.12	−15	9.7	7.7	Farag et al. (2008)
		−1	18.3	26.1	
Lean minced beef meat	13.56	−15 to 65	28–86	50–600	Bedane, Chen et al. (2017)
	27.12	−15 to 65	30–98	60–700	
	40.68	−15 to 65	33–126	90–1200	
Chicken breast (75.5 % of moisture content)	200	−19.4 to −1.3	5–47	0–32	Trabelsi (2015)
Tuna flesh (lean; 70.9 % and 1.0 % of moisture and fat content, respectively)	13.56	−20 to 10	5.4–263.0	2.0–483.9	Llave et al. (2014)
	27.12	−20 to 10	1.7–89.5	1.0–276.9	
Tuna flesh (mid-oily; 61.8 % and 11.0 % of moisture and fat content, respectively)	13.56	−20 to 10	3.7–56.2	1.28–253.9	Llave et al. (2014)
	27.12	−20 to 10	3.4–20.4	0.9–130.9	
Tuna flesh (oily; 44.9 % and 30.6 % of moisture and fat content, respectively)	13.56	−20 to 10	3.7–20.0	1.4–116.1	Llave et al. (2014)
	27.12	−20 to 10	2.6–14.1	1.0–71.9	
Minced fish (76 % and 0.3 % of moisture and fat content, respectively)	27.12	−15 to 10	4–70	0–120	Yang et al. (2019)
Tuna flesh (lean; 72.9 % and 0.5 % of moisture and fat content, respectively)	27.12	−40 to 40	164.7 <sup>a</sup>	552.8 <sup>a</sup>	Chen et al. (2021)
Minced grass carp (80.4 % and 1.0 % of moisture and fat content, respectively)	27.12	−40 to 40	129.8 <sup>a</sup>	307.7 <sup>a</sup>	Chen et al. (2021)

<sup>a</sup>Results shown in Table 2 from Chen et al. (2021) were collected at 20 °C.

The effect of both dielectric constant and loss factor is rather significant since the absorption of electromagnetic energy in high proportion does not directly lead to the conclusion of the higher rate of dissipation. Another combined effect of these two properties lead to the penetration depth. With the physics point of view, when electromagnetic waves strike onto a material, they are absorbed, transmitted, and reflected. The absorption is directly related to the penetration of the electromagnetic energy into the product, and it is defined to be the depth at which the power of the absorbed electromagnetic waves becomes  $1/e$  ( $e=2.718$ ) of what it is at the surface of the product ( $d_p$ , m). Penetration depth as a function of applied frequency and the DPs is given by the equation (Eq. 7) as reported by Von Hippel (1954):

$$d_p = \frac{c}{2\pi f \sqrt{2\epsilon' \left[ \sqrt{1 + (\epsilon''/\epsilon')^2} - 1 \right]}} \quad (7)$$

where  $c$  is the speed of light in free space ( $3 \times 10^8$  m s<sup>−1</sup>) and  $f$  is the frequency (Hz).

### Experimental measurement of dielectric properties

A DP measurement system generally consists of a signal analyzer connected to a sample holder. The signal analyzers used for DP measurements include LCR [inductance (L), capacitance (C), resistance (R)] meters, impedance analyzers,

and spectrum/network/vector analyzers. For property measurements in 1–300 MHz, an LCR meter (works well for 5 Hz–3 GHz) (Izadifar and Baik 2004; Ozturk et al. 2016) or an impedance analyzer (20 Hz–3 GHz) (Boreddy and Subbiah 2016; Jeong and Kang 2014; Llave et al. 2014; Wang et al. 2003) provide accurate results. Spectrum/network/vector analyzers also work well for high frequencies (30 kHz–8.5 GHz) (Zhang et al. 2016; Zhu, Guo, and Jia 2014), but they might also be used to measure DPs in the RF range at a lower accuracy (by using an appropriate test cell) especially for low-moisture food products.

The DP measurement of frozen samples brings an additional challenge since the phase change affects the change in the DPs drastically. At this point, the effect of temperature and frequency have a combined role in this challenge. Despite numerous studies devoted to the measurement of DPs of frozen samples by using an open-ended coaxial dielectric probe kit, Curet, Rouaud, and Boillereaux (2014) reported that this method remains more appropriate for defrosted foods due to their high DP characteristics. While cavity perturbation method seems to be more accurate for frozen foods, requirement of a proper cavity for the measurement brings additional difficulty to the experimental measurement. In addition, for frozen foods, it is necessary to ensure that the frozen samples are kept at a specified temperature (Llave and Sakai 2018). Several studies have reported a jacketed sample holder with a circulating oil/water system to control the sample temperature during the

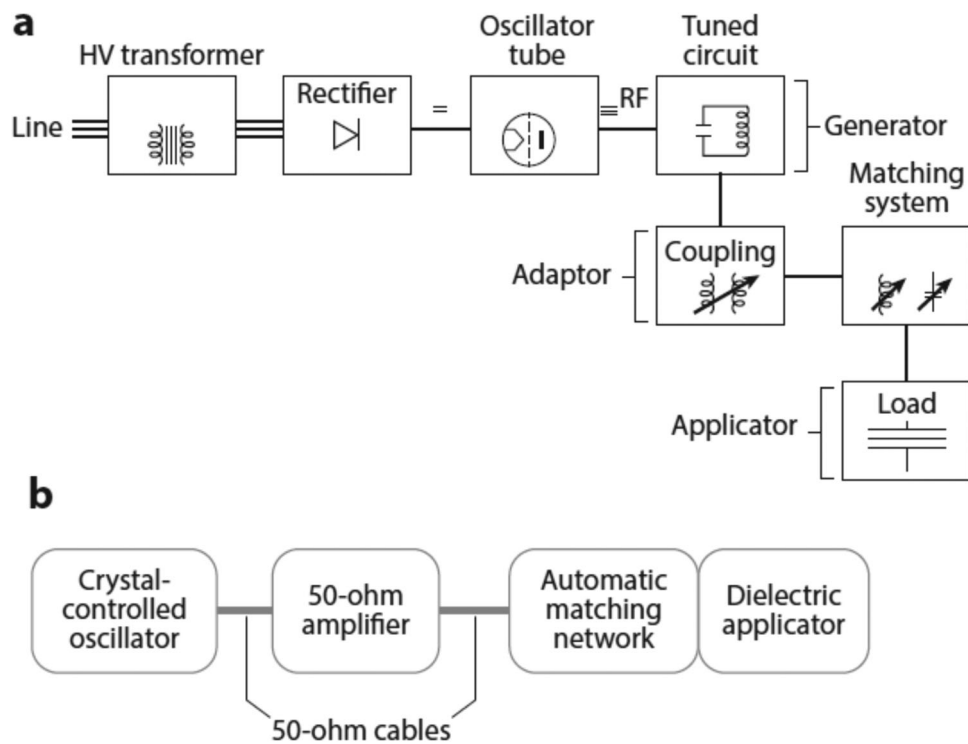


**Figure 3.** Scheme of (a) a typical free-running oscillator (FRO) radio frequency (RF) system and (b) a 50-Ω RF system. [From Jiao et al. (2018) with permission of Annual Reviews].

measurement (Wang et al. 2003). Farag et al. (2008) used a water bath for recirculation of water at a desired temperature through a jacketed sample cup holder. However, as the liquids have different freezing points, below-zero refrigeration of sample containers with water or liquid coolants is somewhat challenging. One work around is to employ a tempered chamber in which the measurement device is placed (Llave et al. 2014; Trabelsi 2015; Wang et al. 2012). Trabelsi (2015) reported that for determination of DPs, the entire assembly—coaxial cable/open-ended probe/stainless steel cup—was placed in a temperature chamber.

For analysis of the DPs at the surface, it is important to ensure the full contact between electrode and the sample surface. This requirement is complicated for frozen samples because the surface would not adhere easily to the surface of the coaxial probe (Liu and Sakai 1999). Besides, if it is not carried out quickly, surface temperature might also deviate from the target measurement temperature. Frozen samples cannot easily attain a good contact between the sample surface and the flat contact-surface of the coaxial probe. The requirement of the probe that the surface flatness of the sample satisfies the flatness condition of the device manufacturer, e.g.,  $2.54 \times 10^{-6}$  m is a significant challenge (Llave et al. 2016). This condition is apparently difficult to attain during sample preparation. The method for fine-tuned roughness correction of the top surface of the frozen samples was successfully used by Liu and Sakai (1999) and Llave et al. (2016). The roughness correction method consists of pressing the surface with a smooth metal at the very early stage of freezing, followed by prompt freezing of the sample in close contact with the metal. Finally, after reaching the final target temperature, the metal is separated from the

surface. This approach improves smoothness of the surface without influencing the structure of the frozen samples (Llave et al. 2014).

### Power absorption

Efficiency of dielectric heating relies on power input, applied frequency, and DPs of the product. Power absorption by the material is described with the following equation (Metaxas 1996):

$$P = 2\pi f \epsilon_0 \epsilon_r'' |\vec{E}_m|^2 \quad (8)$$

where  $P$  is the power absorption by the load per unit volume ( $\text{W m}^{-3}$ ),  $f$  is the frequency of the RF generator (Hz), and  $|\vec{E}_m|$  is the electric field intensity in the load ( $\text{V m}^{-1}$ ) (Jiao, Tang et al. 2014).

### Radio frequency systems

RF systems can be generally divided into two types: free-running oscillator (FRO) systems (also called open circuit RF heating system) and 50-Ω systems (Awuah, Ramaswamy, and Tang 2014).

The open circuit RF systems consist of a high-voltage transformer, a rectifier, an oscillator tube, a tuned circuit, an impedance coupling and matching circuit, and an applicator (Figure 3a). The line power from the AC mains is transformed to a high voltage and converted into DC power by a rectifier. The oscillator uses a thermionic tube, which drives the resonant circuit to generate RF energy at a specific working frequency. RF energy is then transmitted to the

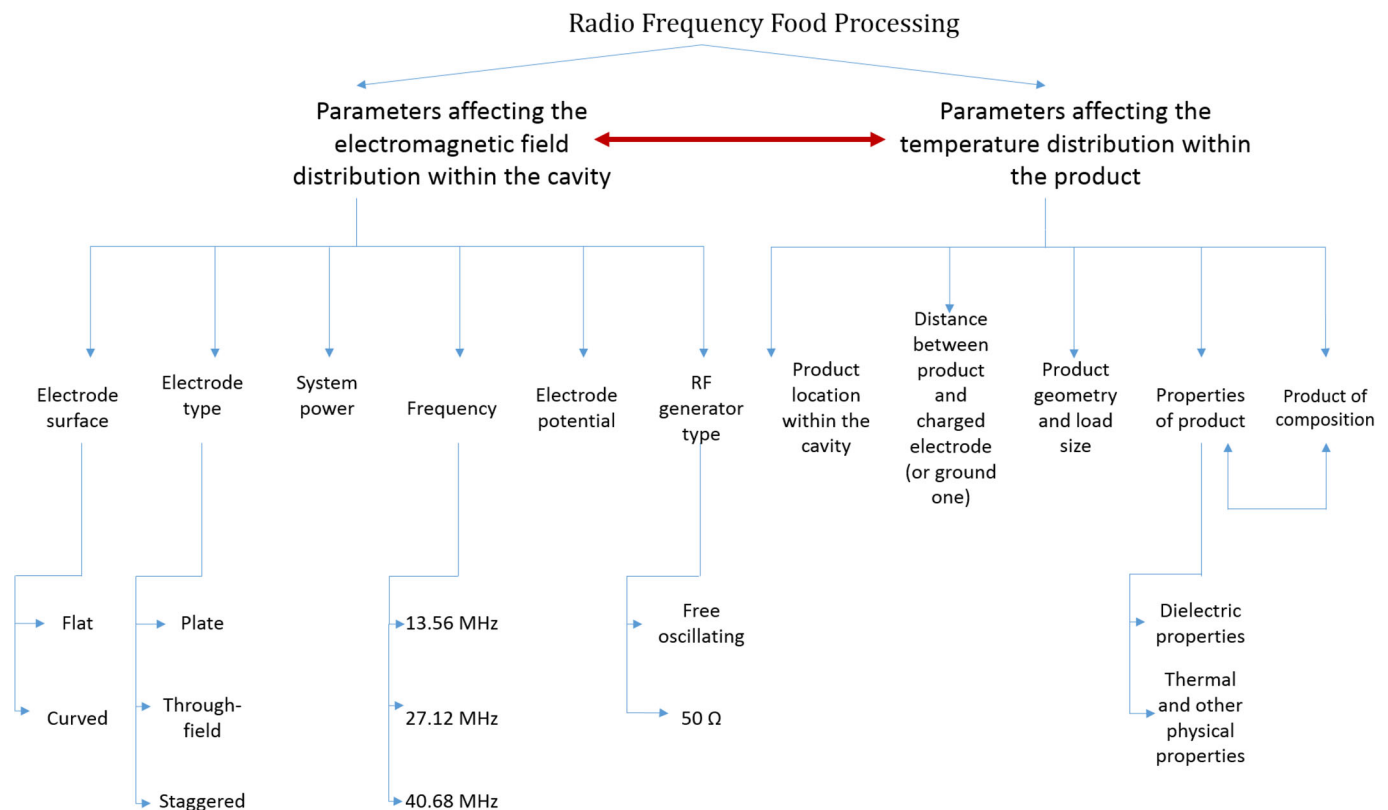


**Figure 4.** Intrinsic factors of an RF food processing affecting the electromagnetic field and temperature distribution.

product load placed between the electrodes, thereby generating heat within the load by dielectric loss (Jiao et al. 2018).

The 50- $\Omega$  RF systems consist of a fixed-frequency crystal-driven oscillator (e.g., quartz), a solid-state amplifier, a dynamic automatic impedance matching network, and an applicator (Figure 3b). The oscillator, amplifier, and matching network are connected with 50- $\Omega$  cables. In 50- $\Omega$  RF heating system, an automatic tuning, as a part of an application circuit, adjusts its overall impedance to 50- $\Omega$  to match the impedance of the generator, thus providing a stable coupling of RF energy and load materials during a stable heating process (Wang et al. 2011). The power consumption and voltage level on the potential applied electrode system are rather easy to determine in these systems compared to the open circuit systems. In the 50- $\Omega$  systems, the voltage level might be maintained at a constant level while the other systems bring a certain challenge to determine the voltage level of the electric potential applied electrode. This challenge leads to certain problems in computational studies since the knowledge of the applied potential must be known for further design—optimization related studies. Therefore, experimental temperature of a material (with its known thermal-physical and DPs) is used to determine the potential of the charged electrode with the presence of a previously developed mathematical model. This model is then applied to determine the potential via a trial and error procedure assuming that the power—potential will not change with the use of different materials under the same processing conditions.

The open circuit RF systems are simple, flexible, and less costly compared to the 50- $\Omega$  systems. Since the 50- $\Omega$  RF heating systems have a higher cost, they are mainly used in

experimental level with an exception of Japan where most of the used devices at industrial levels are 50- $\Omega$  RF heating systems. However, for both RF systems, equipment design requires strict sealing and shielding structures due to that their being subject to a high near-field interference from any radio transmitter operating in the vicinity.

Several companies based in Italy, the United Kingdom, France, the United States of America, Turkey, and Japan have produced commercialized RF systems for thawing/tempering. For example, Yamamoto Vinita (Japan) manufactures ~5–240 kW high-frequency tempering machines using 13.56-MHz RF waves that have a throughput of ~60–4,000 kg h<sup>-1</sup> on thick meat blocks and has applications also on beef, chicken, pork, fish, and seafoods. Stalam (Italy) produces RF defrosting equipment with a power of ~3–105 kW and frequency of 27.12 MHz for meat, fish, and vegetables. It has a maximum throughput of 2,500 kg h<sup>-1</sup> when tempering frozen meat from -25 to -5 °C. In addition, SAIREM SAS (France) with 50- $\Omega$  RF technology manufactures ~6–120 kW using 27.12 MHz to defrost: seafood, meat, vegetables, and ready meals. While the main industry aim for SONAR (Turkey) is not the food processing industry, their 27.12 MHz free running oscillator systems have found a certain application range for academic research in the last decade.

RF applicators are basically the interface between a RF generator within the RF cavity and the food product. Bernard, Jacomino, and Radoiu (2015) gives a detailed information about RF applicators. Within staggered through-field electrode systems, bottom electrode (array of electrodes in the form of rods in the current system) is charged while top electrode serves as ground, opposite to the mostly used



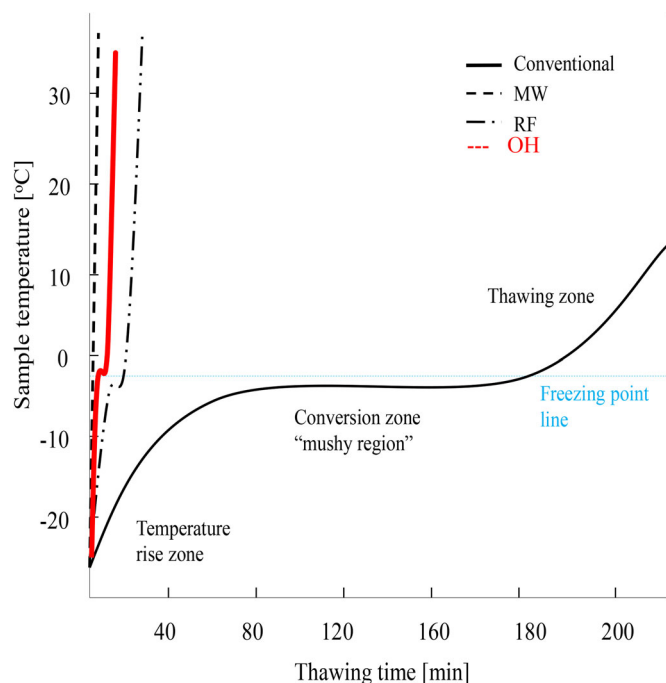


**Figure 5.** Typical thawing curves of frozen tuna samples for different thawing methods: Conventional (natural-convection air), radio frequency (RF) heating, microwave (MW) heating, and ohmic heating (OH). [Adapted from Llave and Sakai (2018)].

through-field electrode applicators (where metal plates serve to be charged and ground electrodes). There are also design of the staggered through-field electrode systems where the top electrode is still the potential applied one. In through field RF systems, however, the upper electrode is the charged one, and these systems are accepted to have the simplest capacitive configuration. The staggered through field electrode applicators, on the other hand, are arranged above or below of the processed material as indicated above.

RF thawing can be performed in both batch and continuous modes, and it can also be carried out inside the packaging materials, such as carton boxes and polyethylene bags. The mode of operation, either in batch or continuous, also affects the temperature distribution and heating rate in the food sample (Guo, Mujumdar, and Zhang 2019).

As explained in this section, there are various factors affecting the electromagnetic distribution inside an RF cavity and the temperature change/distribution inside the processed products. These two distributions (electromagnetic distribution and temperature distribution) also interact mutually where the change in the temperature due to the absorption of electromagnetic energy results in the specifically change of the DPs. This eventually leads to the change in the electromagnetic energy absorption distribution inside the product. Figure 4 summarizes possible intrinsic factors of an RF food processing affecting both the electromagnetic field and temperature distributions.

### Conventional thawing/tempering vs. electro processing thawing/tempering

Thawing by itself is a slow process and takes place gradually over a range of temperature (Chamchong and Datta 1999).

In Figure 5, the typical thawing curves for different electro processing thawing methods are shown: RF heating, MW heating, ohmic heating (OH), and conventional (natural-convection air) heating. The temperature profiles corresponded to the center positions of small frozen tuna samples, 200 g in block shape for RF thawing (Llave et al. 2014), 195 g in cylindrical shape for MW thawing (Llave et al. 2016), 150 g in block shape for OH thawing (Liu et al. 2017), and 200 g in block shape for conventional air thawing (unpublished work). Initially the temperature rise is very rapid because of the presence of an (high thermal conductivity) ice layer around the surface of the frozen sample. Thermal conductivity of ice is also higher than that of water leading to a rapid heat transfer in the frozen sample. Upon the conversion of ice over the surface to water and subsequent conversion within the sample result in decreases in the heat transfer rate (Llave and Sakai 2018). While the latent heat of fusion is absorbed, a steady plateau is observed with no-changes in temperature, and a complete thawing is achieved when all the ice is converted into water. A significant temperature increase is then observed. This is a typical thawing process observed for conventional thawing systems where the heat transfer medium is either air or water with a limited convective heat transfer rate. Application of MW gives a rather faster thawing due to the higher frequency applied compared to the RF application. This results in higher power absorption by the product with a better temperature increase. However, the control of this high power is questionable as explained before, and it comes with an expense of a significant temperature non-uniformity. Although OH is usually applied for smaller solid samples than by RF heating, most of the energy is transferred to the food product in OH (beyond 90% of energy efficient) leading to a higher heating rate compared to RF. However, the essential contact between sample surface and electrodes is sometimes lost due to drip losses during OH defrosting applications. Heating rate for the various thawing process might be  $MW > OH > RF > \text{convection air}$  with respect to the thawing time.

The main goal of suitable thawing is to cause the least amount of damage with the shortest possible thawing time. An RF system has the potential for use in achieving these goals for industrial thawing operations (Yang et al. 2019). With the rapid and volumetric heating behavior of RF application, it is also possible to achieve thawing in shorter times compared to the longer times of a conventional processes. This then leads to the minimized risk of degradation of the quality factors (Farg et al. 2011; Uyar et al. 2015). However, while a tempering process is rather convenient to achieve with RF application, thawing brings additional challenges due to the reasons explained in “Introduction.” Tempering is about to increase the temperature of the product under the thawing front temperature. Due to the limited changes in the DPs before the phase change, temperature uniformity is achievable except at the corners and edges (due to fringing and the strong interaction of the electromagnetic field with the magnet-like effect). For thawing however, the temperatures over the thawing temperature

need to be achieved, and within this range, temperature increase might be uncontrollable due to a drastic increase of the DPs at this temperature range. Therefore, during thawing, it is necessary to better understand the electromagnetic field interaction within the cavity and through the product. It is also important to consider the balance between thawing time, food safety, and the energy usage to decide upon the proper process and optimal process parameters (Bedane, Marra, and Wang 2017).

For MW processing, as the penetration depth depends upon the applied frequency and DPs, local thermal runaway has a high possibility to occur. The higher frequency affection of the power absorption also plays a significant role on this issue. That means, due to the limited penetration depth—contrary to the literature focusing of the volumetric heating, boundary layers are likely to get affected by the MW process due to limitations in the penetration depth whereas the inner layers remain frozen and will be thawed under the significant effect of conventional conduction (heat transfer from outer thawed surfaces to the inner volume). Due to the fact that the heating gradient with MW is larger than that for conventional conduction, the boundary layers will heat up faster than the inner layers. This phenomenon is enhanced by that liquid water absorbs more energy than ice—thus the term thermal runaway is faced (Llave et al. 2020). Common penetration depths for private use MW processes (2450 MHz and 1–2 kW power, Choi et al. 2015) are not more than a few centimeters—enough for domestic applications, but most likely not for industrial applications. Therefore, for industrial processes, lower frequencies are preferred (e.g., 915 MHz) with a higher power (e.g., 5–10 kW) (Chen, Tang, and Liu 2008).

RF, with the right power input, is supposed to be a better controlled process in terms of overheating and uniform temperature distribution compared to a MW process. For example, recently Chen et al. (2021) has been compared the temperature distributions of tuna and its model food made from grass carp mince and additional ingredients at the top surface, bottom surface and longitudinal sections after RF and MW tempering, concluding that samples were tempered unevenly in MW experiments because the penetration depth of the thawed parts in the samples decreased dramatically which caused localized heating in the samples. Therefore, local thermal runaway still imposes a disadvantage. However, since the penetration depth of RF is greater than that of the MW, RF thawing can result in a more uniform heating compared with MW thawing (Llave and Sakai 2018) with a more controllable power absorption due to the lower applied frequency.

## Radio frequency thawing/tempering applications

### Historical review

RF thawing is a rather rapid thawing method that attracted more attention by the literature and industry in recent years. Initial attempts for RF application, however, lies back to 1940s where its potential for thawing frozen meat, fish, and vegetables was explored with a little reported information in

the published literature. Perhaps the earliest RF research on thawing was reported by Cathcart and Parker (1946) where RF thawing process was applied to frozen fish, eggs, fruits, and vegetables. It was determined that the RF application at 14 to 17 MHz could significantly reduce the thawing time. Bengtsson (1963) reported some of the earliest DP data in the frozen region for lean beef and cod fish at several RF frequencies (10, 35, 100, and 200 MHz) and temperatures (−25, −10, −5, and 10 °C) during a defrosting process. Although commercial RF thawing/tempering equipment has been used for decades, rather significant research findings on meat and fish thawing/tempering have been published within the last decade or so. These studies used RF systems to meet the increasing requirement for food safety, to reduce food waste, and to provide high-quality products for the consumer market (Jiao et al. 2018).

### Recent radio frequency applications for thawing/tempering

#### Seafood

While thawing itself is a challenging process, it brings additional concerns for the case of marine products due to the delicacy in their physical—structural properties. Gökoğlu and Yerlikaya (2015) reported that the thawing rate should be quick to avoid the water changing its original position and causing drip loss (to also prevent the dry, stringy texture, and a less tasty fish). In addition, the target thawing temperature should be low, otherwise microbiological and enzymatic reactions would be accelerated at higher temperatures. Nutrient loss also easily occurs along with drip loss, that is, water-soluble proteins, vitamins, and minerals all are found in the drip. Protein oxidation and denaturation would also be increased with the formation of disulfide bonds. The lipid oxidation possibility might bring about nutritional and textural changes. Furthermore, color changes in fish and crustaceans during thawing can be a problem. Many reactions occur easily in fatty fish and cause rancid odors and flavors (Gökoğlu and Yerlikaya 2015).

Llave et al. (2014) determined the DPs of three types of frozen tuna muscles in the tempering temperature range and studied the efficacy of RF tempering of frozen tuna blocks. The effects of RF thawing (in the frequency range of 13.56 to 27.12 MHz) were compared with air thawing of tuna blocks. Like the effects of RF thawing with other food products, thawing time was threefold less than that of air thawing and using an electrode size comparable to the sample surface achieved a better heating—temperature uniformity. The benefit of RF thawing also depended on the fat content of the frozen fish muscle. The fish muscle that contained less fat would lead to a process with more uniformity in temperature compared to fatty fish muscle (Llave et al. 2014) due to the more uniform composition and DP distribution within the product.

Sato, Yamaguchi, and Nakano (2016) thawed fish eggs using a RF frequency system at  $100 \pm 10$  MHz. Thawing of fish or whale meat, frozen minced fish meat, and meat or minced meat were also tested. Output of the applied

thawing device was reported to be adjusted to an appropriate level to prevent the overheating of frozen food. This method was reported to achieve a uniform temperature distribution and rapid thawing while maintaining the quality of the product. Sato, Yamaguchi, and Nakano (2016) claimed that this technique was suitable for thawing marine products where fresh and delicate tastes need to be maintained.

Palazoglu and Miran (2017) conducted a tempering process to frozen shrimp blocks by MW and RF methods. They pointed out that MW tempering showed a shorter tempering time (10 and 4 min for 500 W and 1 kW to  $-5 \sim -3^{\circ}\text{C}$ ) compared to RF tempering (11 and 7 min for the electrode gap of 160 and 150 mm to  $-5 \sim -3^{\circ}\text{C}$ ). However, local overheating of the frozen block was found to occur during MW tempering at all power setting while RF tempering resulted in a uniform overall temperature distribution with no local overheating.

Yang et al. (2019) investigated the characteristics of RF thawing and sought to determine the optimal conditions for RF thawing by clarifying the temperature distributions in blocks of frozen minced fish. A sharp increase in DPs ( $\varepsilon'_r$  and  $\varepsilon''_r$ ) at 27.12 MHz frequency (from  $-3$  to  $0^{\circ}\text{C}$ ) and a pronounced decrease in the penetration depth from  $-15$  to  $-5^{\circ}\text{C}$  were observed. Results showed that electromagnetic waves at this frequency could penetrate the samples easily, and the heating uniformity might be improved at both ranges of temperature. For the size of frozen minced fish blocks that are commonly used in the industry ( $25 \times 15 \times 5$  cm), the most suitable electrode gap for thawing was suggested to be 16 cm, because it produced a more uniform temperature distribution and a better gel strength. In addition, to further reduce the edge-effect of the electromagnetic field, it was feasible to increase the sample size so that increasing the sample's bottom areas (to sizes such as  $25 \times 35$  cm) might become the direction for future industrial improvement.

### Beef

RF defrosting applications of frozen beef products have been the most popular applications reported in the literature. Farag et al. (2008) used a pilot-scale 50- $\Omega$  RF heating system (27.12 MHz) for tempering beef meat blends and determined the optimum RF tempering parameters for lean and lean/fat mixture (50:50, lean/fat) to achieve a temperature range from  $-2$  to  $-5^{\circ}\text{C}$  to be 11 min for 500 W, and 11 min for 400 W for the case of fat blends. Compared to the conventional air heating, RF heating reduced the tempering time approximately 30-fold time with a 9-fold power consumption decreased. It resulted in an increased temperature uniformity at the endpoint of RF tempering. The results also suggested that improving the homogeneity of sample composition could enhance thawing uniformity further with respect to the temperature distribution. Furthermore, the required energy consumption decreased significantly as indicated, and the drip and micronutrient loss values (Na, Mg, K, Ca, and Fe) compared to air thawing were also reduced (Farag et al. 2009).

A significant reduction in tempering time along with a comparable uniformity of temperature distribution was reported by Farag et al. (2011) when 400 W RF tempering was employed for 4-kg blocks of lean beef meats. However, when higher temperatures ( $-1$  to  $5^{\circ}\text{C}$ ) were targeted for the purpose of a thawing process, a considerably longer time (35 min higher compared to the previously tempering result) was required to complete the process through the phase change zone. Bedane, Chen et al. (2017) explored the DPs of lean minced beef meat and found that the gap between electrodes with RF thawing was associated with the heating uniformity.

Uyar, Erdogdu, and Marra (2014) demonstrated the effect of sample size and its orientation between the RF electrodes on the temperature evolution. In a fixed electrode gap, the smaller the load volume the slower the heating rate of the sample due to the behavior of the electric field. The smaller sized samples, compared to the electrode gap, resulted in lower power absorption compared to the MW processing. However, when the electrode gap was limited, the smaller volume samples heated in an accelerated heating rate due to the deflection of the electric field through the bottom-top edges of the sample. This increased the power absorption of the sample with an increase in its temperature. Results of this study demonstrated a significant effect of load volume during RF processing, and that it was possible to obtain an optimal design of an RF cavity to lead to a higher heating efficiency by changing the distance between the electrodes.

### Pork

Choi et al. (2017) investigated the effect of various tempering methods (forced air, water immersion, RF, and MW) on tempering rate of frozen pork loin ( $100 \times 100 \times 70$  mm). A 19-fold reduction in tempering time (time to bring pork loin from  $-20$  to  $-2^{\circ}\text{C}$ ) was observed with the RF system when compared to forced air treatment. MW tempering (2.45 GHz) was, however, found to be the fastest method of all, but less uniform internal sample temperature distribution compared to RF tempering. Zhu et al. (2019) explored the effects of different tempering methods and end-tempering temperature on pork quality (1 kg frozen lean pork samples in cuboid shapes), treated under RF tempering (3 kW, 27.12 MHz) including water tempering and air tempering from  $-22$  to  $-1^{\circ}\text{C}$  and  $-4^{\circ}\text{C}$ , respectively. Results showed that both tempering methods and tempering temperature had significant ( $p < 0.05$ ) effects on pork quality. The tempering time required for water and air tempering were about 9 and 17 times longer than RF tempering to reach  $-1^{\circ}\text{C}$ , respectively. From the tempering temperature point of view, when tempered to  $-1^{\circ}\text{C}$ , no significant effect was found in the physical and chemical properties of pork samples compared to the tempering to  $-4^{\circ}\text{C}$  except for the increased drip loss, cook loss, and the decreased pH.

### Poultry

Yu et al. (2005) evaluated the effects of tempering temperature on the quality of pre-rigor frozen chicken. Chicken



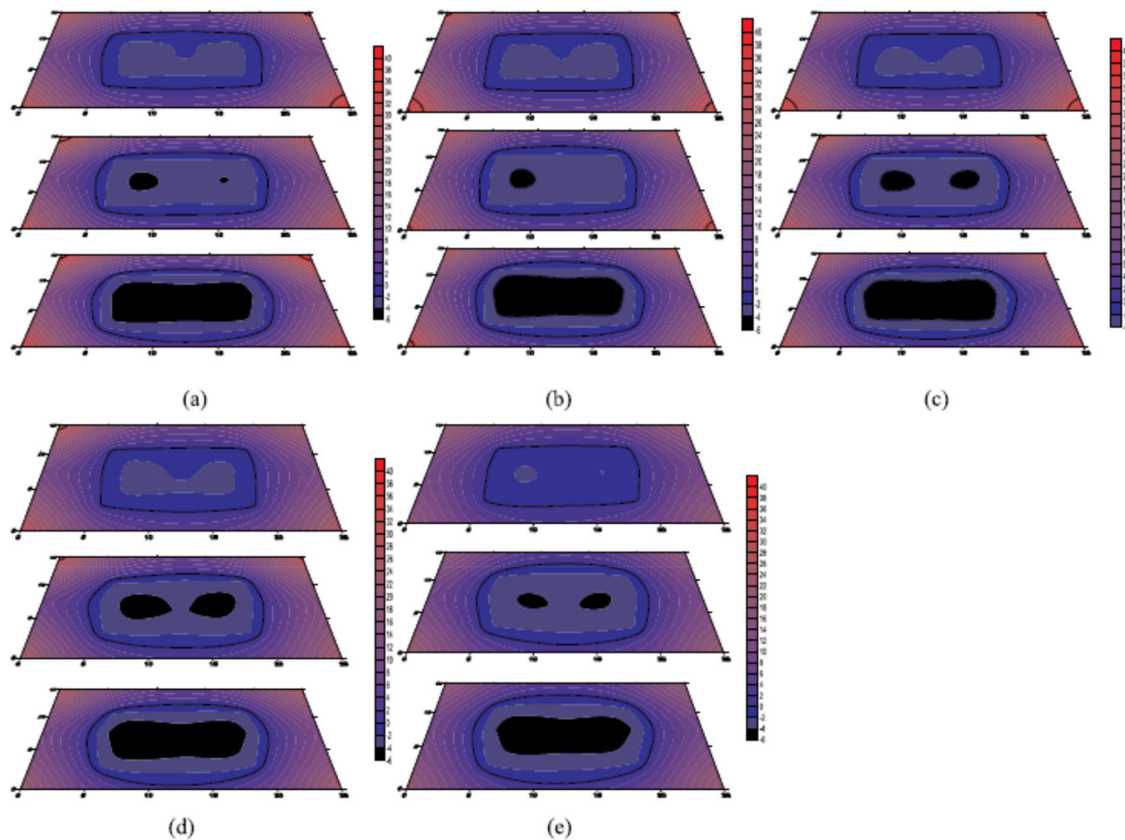


**Figure 6.** Temperature distributions within frozen minced fish with use of different electrode gaps: (a) RF 14 cm, (b) RF 16 cm, (c) RF 18 cm, (d) RF 20 cm, and (e) RF 24 cm. (The temperature data obtained were plotted in Surfer.) [From Yang et al. (2019) with permission of Elsevier].

samples were frozen at  $-20^{\circ}\text{C}$  and tempered at 0 and  $18^{\circ}\text{C}$ , respectively. Tender meat was obtained with tempering at  $0^{\circ}\text{C}$ . While RF thawing studies for poultry are limited in the literature, in the study by Bedane et al. (2018), thawing temperature uniformity with changes in quality parameters during RF thawing of frozen chicken breast were investigated. Complete RF thawing to  $-0.73 \pm 0.79^{\circ}\text{C}$  using 65 mm electrode gap in a staggered through system took 40 min compared to 18 h of conventional thawing with significantly reduced drip losses (0.32 compared to 4.84%) and improved textural attributes.

## Current issues

### Arcing and cause of arcing

Arcing (flashing) is a potential problem in all RF processing and is not well understood yet (Jiao et al. 2018). It generally occurs when the RF potential between two points exceeds the voltage that those points can withstand without causing the material separating them (usually air or product) to break down. The energy contained in such a sustained arc is more than enough to set the product on fire as well as to cause burning of the conveyor band and damaging the components of the system. Therefore, a suitable arc detection system should always be employed in all RF systems. However, this is not always incorporated by all manufacturers in practice, and arcing might be observed occasionally.

To avoid the arcing problem, it is essential to start with a product as homogeneous as possible in composition and size (especially height) (Jiao et al. 2018). Random irregularities over the surface and edges are likely to absorb higher energy resulting in arcing. Zhao et al. (2000) reported that arcing gets more complicated due to surface irregularities and edge effects of the food especially that might come closer to or in contact with electrodes. More detail of the basic causes of Arcing can be found in previous published works in this field (Awuah, Ramaswamy, and Tang 2014; Jiao et al. 2018).

### Non-uniform heating

Another major challenge for RF heating, as also indicated above, is the non-uniform heating caused by the unavoidable uneven distribution of the electromagnetic field in the material and within the cavity. The effect due to the product is inevitable for frozen foods (Guo, Mujumdar, and Zhang 2019) due to the significant difference in the DPs of thawed and frozen regions. Therefore, it is essential that the electromagnetic field should be uniformly distributed within the food material's geometry to ensure uniform heating. In addition to DPs and the electromagnetic field intensity, the heat capacity and bulk density of the sample were also found to influence the heating rate of foods significantly (Zhang, Jiang, and Lim 2010). Thus, when the non-uniform food is heated in a RF system, it will have a non-homogenous heating rate in different parts, resulting in non-uniform

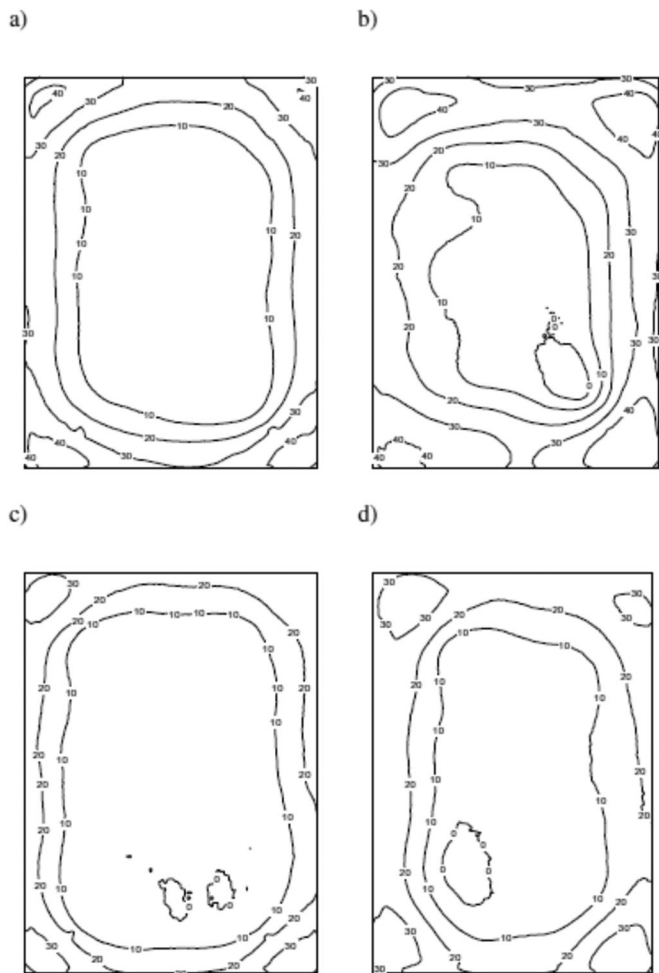


**Figure 7.** Temperature distributions ( $^{\circ}\text{C}$ ) on top and middle surfaces of RF thawed lean beef meat block at 10 cm electrode gap after 17 min treatment. Stationary: top surface (a), middle surface (b), moving at  $3\text{ m h}^{-1}$ : top surface (c), and middle surface (d). [From Bedane, Chen et al. (2017) with permission of Elsevier].

temperature distribution. The parts of the food material at higher temperature will heat faster, resulting in a “thermal runaway” effect (Guo, Mujumdar, and Zhang 2019). It can be observed in the temperature distributions shown in Figure 6, for the case of blocks of frozen minced fish during RF thawing at different electrode gaps (Yang et al. 2019). They sought to determine the optimal conditions for RF thawing by clarifying the temperature distributions.

Due to the intrinsic properties of the dielectric material, fringing field formation around and inside the food product is the cause of non-uniform heating in foods (Figure 2) (Margulies 1984). To balance out the fringing field effect, uniformity improvement methods suited to different products were developed. Some of these experimental challenges are discussed in the following sections and the mathematical approaches in the computer simulation section.

### **Solutions to improve radio frequency heating uniformity**

Various techniques have been proposed to improve heating uniformity during RF processing. The electromagnetic field of RF equipment between two parallel electrodes was found

to depend on the geometry of, especially, the potential applied top electrode. In some studies, the electrode geometry was modified, and this led to a reduction of the fringe effect (where non-perpendicular electromagnetic waves applying over the sample surface) from the edges of the electrode, thus improving the heating uniformity (Erdogdu et al. 2017; Llave et al. 2015). Movement and rotation of sample were also found to have an ability to redistribute the electromagnetic field and heat within the food product, thus improving the RF heating uniformity (Bedane, Chen et al. 2017; Bedane, Marra, and Wang 2017; Erdogdu et al. 2017).

Subsequently, adjusting output energy during RF heating was demonstrated to have an ability to avoid local overheating and improve the heating uniformity. Fiore et al. (2013) reported that, by adjusting the output power of RF generator, the energy absorption of food materials can be controlled to further avoid the local overheating. Additionally, Hansen et al. (2006) and Farag et al. (2011) suggested that during the pulse mode, the holding period between RF treatments allows the heat in different positions of the food to dissipate and become more equal throughout, which can be an efficient way to improve the heating uniformity. Another approach is surrounding the food with a cooling medium. It can reduce the temperature variation in the food or allows holding at a desired temperature. The selection of cooling medium depends on properties and treatments of the sample.

Farag et al. (2011) reported that RF (27.12 MHz, 600 W) non-continuous power-time combinations for thawing lean meat at 400 W for 35 min (20 min on, 10 min off, and followed by 15 min on) was reported to achieve a better heating uniformity compared to continuous RF thawing method. In addition, using the package or container that have DPs similar to the food materials’ can also be an efficient way to improve the uniformity. Recently, Huang et al. (2016) investigated the effects of using polystyrene container to improve heating uniformity for low-moisture agricultural products. Uyar, Erdogdu, and Marra (2014) placed the food material in the middle of the electrodes to avoid the electromagnetic field concentration at contact surfaces and modified the volume to achieve a uniform distribution of electromagnetic field within the food to improve the heating uniformity. Improving the heating uniformity during an RF thawing/tempering process is the significance challenge, and three of the most successfully and documented approaches are discussed below in detail.

### **Stationary vs continuous radio frequency systems**

Bedane, Chen et al. (2017) used a pilot-scale RF (27.12 MHz, 6 kW) to thaw lean beef meat block ( $19 \times 12.5 \times 5.5\text{ cm}^3$ ) under batch (static sample between electrodes) and continuous (sample moving between electrodes along the RF system) conditions, respectively for the same electrode gap. It was determined that the temperature distribution of beef samples after a batch mode tempering process was between  $-0.2$  and  $28.4^{\circ}\text{C}$ , while that was  $-1$  to  $12.8^{\circ}\text{C}$  after a continuous process. In addition, it was reported that thawing of frozen lean beef meat blocks on moving conveyor belt



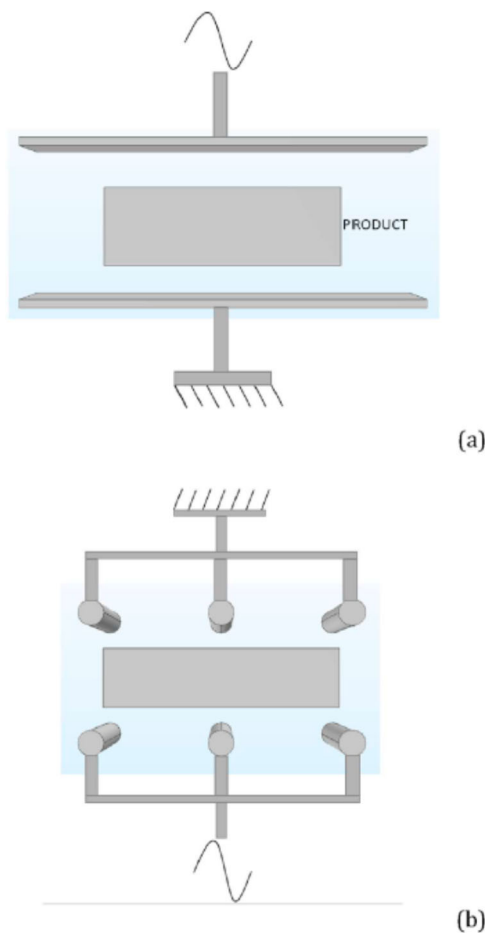


**Figure 8.** (a) Through field and (b) staggered through field electrode principle used in a radio frequency system (Modified from Bernard, Jacomino, and Radoiu 2015). [From Bedane et al. (2018) with permission of Elsevier].

slightly improved the heating uniformity across the food product (see Figure 7). Average temperatures of  $-0.2 \pm 1.5^\circ\text{C}$  and  $0.4 \pm 0.7^\circ\text{C}$  were achieved at 17 min of thawing time using static conditions and moving on conveyor belt at  $3\text{ m h}^{-1}$ , respectively. These studies revealed that although RF tempering is beneficial in faster heating, temperature uniformity is still affected by many factors including end-tempering temperature, which would further influence meat quality.

#### Staggered through field electrode systems

Most of the reported studies mentioned in the previous section, have used the plate electrode systems where the top electrode was the charged one while the lower one was the ground electrode. Until recently, this electrode design was the mostly applied while a recent study (Bernard, Jacomino, and Radoiu 2015) introduced the use of a staggered through electrode RF system. In a staggered through field electrode system, the bottom electrode (set of rods) is the charged one while upper one (set of rods) is the ground (Bedane et al. 2018). These systems, compared to the stray field electrode applicators where charged and ground electrodes are placed next to each other below the product (Figure 8), enables thicker materials to be processed (Bernard, Jacomino, and Radoiu 2015). Stray field electrode applicator RF systems are

more suitable for thin layer products, and in these systems, the electrodes in the form of rods are placed below the product. Charged and ground electrodes are placed next to each other in these systems, and the generated electric field has a limited effect on the above placed product. That would be the reason why the stray field electrode applicator systems would fit better for thin layer products.

In a staggered through field electrode systems, depending upon the applied potential and the distance between the electrodes, thicker materials might be easily processed since the electric field moves from bottom to the upper ground electrode covering the sample between them in a similar way to the through field systems. Besides, the space between the charged electrode and the sample becomes comparatively short. Bedane et al. (2018) investigated the electric field distribution in a staggered through-field electrode RF system and thawing temperature uniformity with changes in quality parameters during RF thawing of frozen chicken breast. Higher electric field intensity was observed at center and middle edges of the bottom electrode of the system.

#### Novel approaches in radio frequency electrodes design

The geometry and configuration of the electrodes might also affect the temperature distribution during RF thawing process due to the changes in the electric field distribution. Kim et al. (2016) investigated the thawing of pork meat using curved shape charged—top electrode considering different temperatures in the cavity and reported that use of an electrode in a geometry resembling the product together with lowered temperature in the cavity improved the temperature uniformity. Kim et al. (2016) found that the edges and corners of cylindrical pork samples were over  $20^\circ\text{C}$  when to the center reached  $-4^\circ\text{C}$  in a flat—electrode RF heating system. Curving the top flat electrode to fit the cylindrical pork sample could significantly improve the temperature uniformity.

Choi et al. (2017) reported the quality characteristics of frozen cylindrical pork loin evaluated following different tempering methods: 27.12 MHz curved-electrode RF at 1000 and 1500 W and forced-air convection (FC) or water immersion (WI) at  $4^\circ\text{C}$  and  $20^\circ\text{C}$ . FC tempering at  $4^\circ\text{C}$  was the most time-consuming process, whereas 1500 W RF was the shortest. They reported that curved-electrode RF tempering showed better drip loss results compared to FC and WI. Furthermore, curved-electrode RF tempering showed a more uniform temperature distribution, allowing cylindrical frozen pork loin meat to be processed in a more homogeneous manner. Therefore, for practical applications, curved-electrode RF tempering seems to have a potential advantage to achieve shorter tempering time with smaller processing cavity and quality maintenance for cylindrical-shaped meat blocks in the meat processing industry (Figure 9).

#### Mathematical modelling and simulation

A remarkable study by Marra et al. (2007) for RF heating was one of the pioneering works in the food processing

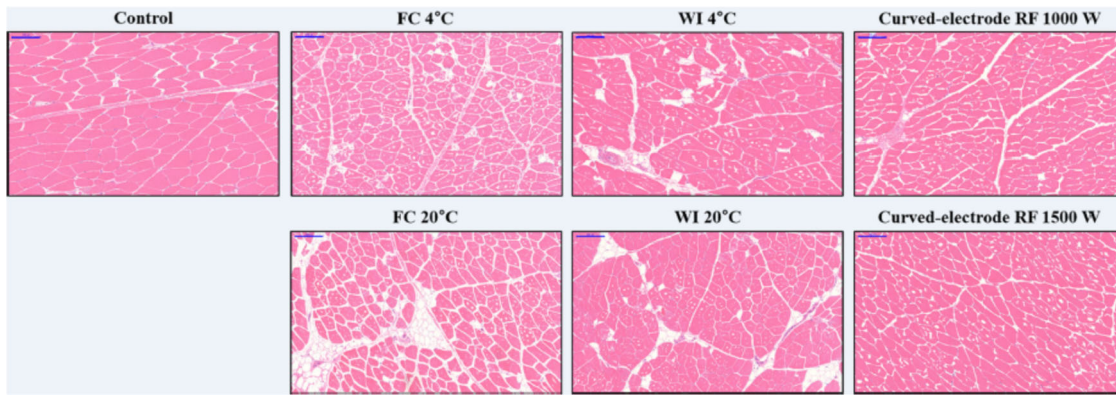


**Figure 9.** Light microscopy images of transverse sections of cylindrical pork loin samples treated with different tempering conditions. The magnification was  $\times 10$ , and the scale bar indicates  $200\ \mu\text{m}$ . FC, forced-air convection; WI, water immersion; RF, radio frequency. [From Kim et al. (2016) with permission of Springer].

literature. Following the approach introduced in this study, the published literature focused on computer modeling techniques for RF defrosting applications have advanced greatly in the last decade also due to the increase in the computational power and improvements in commercial software (Erdogdu et al. 2017; Llave et al. 2015; Uyar et al. 2015; Zhang et al. 2020). The most relevant mathematical modeling approaches to improve heating uniformity for thawing—tempering purpose has been summarized in Table 3.

It is evident that most of the researchers conducted comprehensive studies with the FEM based software COMSOL MultiphysicsR (previously named FEMLAB). Rather easy-to-use interface of this software largely simplified computations and reduced the computational time. The literature studies also showed that the heating pattern of food products subjected to RF can be predicted by computer modeling if parameters and conditions are properly set. According to Guo, Mujumdar, and Zhang (2019), with the help of a mathematical modeling approach and resulting simulation, the electromagnetic field within the cavity can be predicted and modified to improve the uniformity of RF heating. This can be carried out by adjusting the position, geometrical features of the product, as well as the surrounding space of the samples (Ferrari et al. 2016; Huang et al. 2016). Therefore, mathematical modeling has been proven to be an efficient tool to demonstrate the electric field and temperature distribution, test new strategies, optimize parameters, and design appropriate RF treatment conditions as well as to help develop heating uniformity improvement methods (Jiao et al. 2018).

However, the modeling of defrosting process using RF heating has been reported to be a challenging work. Yang et al. (2019), reported that the presence of water during the thawing phase transition changes minced fish from a low-moisture food into a high-moisture food, and this change in moisture content is one of the factors affecting the non-uniformity of temperature distribution. In modeling of a defrosting process, the major challenge is the presence of the moving boundary condition, which leads to a complex interaction of the thawing front, temperature profiles and absorbed energy within the sample (Rattanadecho 2004). Llave and Sakai (2018) explained that thawing happens over an extended temperature range and in multicomponent

samples like food, solid and liquid phases coexist in a heterogeneous region known as the mushy zone. This complicates the computer simulation work since variations in thermophysical properties in the phase transition region also increase the complexity of a RF defrosting simulation. In this section, the progress of computer simulations related to RF thawing/tempering applications is discussed.

### Basics in computer simulation of radio frequency defrosting process

RF heating is a complex, multi-physical process that involves transfers of both electromagnetic energy and heat. The coupled electro-thermal problem for computational model of an RF process becomes more complicated for simulation of thawing since the phase change process requires dealing with evolving large latent heat over a small range of temperature (Huang et al. 2016). Two of the significant works on this front were introduced in the last 5 years (Uyar et al. 2015; Llave et al. 2015) where a detailed information about the governing equations, initial—boundary conditions and physical properties were reported.

### Governing equations

**Electromagnetics.** The electromagnetic field distribution in space and time of electromagnetic waves like RF waves is governed by Maxwell's equations (shown in “Dielectric properties of frozen foods”). While the solution of the Maxwell's equations are required to determine the electromagnetic field distribution within the RF cavity, with a quasi-static approximation of the Maxwell's equations, the Gauss law might be derived due to the longer wavelength of the RF compared to the cavity size simplifying the solution to Eq. (9):

$$\nabla(\varepsilon \cdot \vec{E}) = 0 \quad (9)$$

where  $\varepsilon$  is the permittivity of the load (relative permittivity related to dielectric constant and dielectric loss factors) and  $\vec{E}$  is the electric field vector.

**Heat generation.** The absorbed power per unit volume ( $P$ ,  $\text{W m}^{-3}$ ) in the material is directly proportional to the square of the electric field strength ( $E$ ,  $\text{V m}^{-1}$ ), the  $\varepsilon''_r$  of

**Table 3.** Mathematical modeling approaches to improve heating uniformity during radio frequency heating.

Food material	Radio frequency system properties	Software used	Effect	Reference
Meat batters	27.12 MHz 50 $\Omega$	Femlab 3.1 (COMSOL AB, Stockholm, Sweden)	Pioneering study for the RF heating modeling	Marra et al. (2007)
Lean beef	27.12 MHz 50 $\Omega$	Heat Transfer Module and the ACDC Module of a finite element-based software—COMSOL (COMSOL V. 3.5, COMSOL AB, Stockholm, Sweden)	During RF heating the power absorption is strongly dependent on the sample size.	Uyar, Erdogdu, and Marra (2014)
Minced lean beef	27.12 MHz, 2 kW—free running oscillator system	Heat Transfer Module and the ACDC Module of a finite element-based software—COMSOL (COMSOL V. 4.3b, COMSOL AB, Stockholm, Sweden)	During RF heating the power absorption is strongly dependent on the sample size.	Uyar et al. (2015)
Minced lean beef	27.12 MHz, 12 kW, 50 $\Omega$ RF system	COMSOL Multiphysics® (COMSOL Multiphysics 4.2, Burlington, MA, USA)	Influence of sample thickness (40, 50, and 60 mm), size ( $160 \times 102 \times 60 \text{ mm}^3$ , $220 \times 140 \times 60 \text{ mm}^3$ , and $285 \times 190 \times 60 \text{ mm}^3$ ), and shape (cuboid, trapezoidal prism, and step) on tempering uniformity	Li et al. (2018)
Lean tuna fish	13.56 MHz, 50 $\Omega$	3D geometric model using FEMAP (V. 10.3; Siemens PLM Software, Plano, TX), Photo-Wave-j $\omega$ (version 7.2; Photon Co., Kyoto, Japan) for analysis of the electromagnetic field, and Photo-Thermo (Photon Co.) for the heat transfer analysis	To improve uniformity thawing quality, the electrode should be designed to be similar in size to the samples.	Llave et al. (2015)
Lean tuna fish	27.12 MHz, – free running oscillator system	COMSOL software (V. 5.1, COMSOL AB, Stockholm, Sweden) with moving mesh module	The model considers the movement of the RF electrode and the effects of temperature and electric field changes.	Erdogdu et al. (2017)
Minced fish	27.12 MHz, 6 kW	COMSOL Multiphysics® (V. 5.3 COMSOL Multiphysics, Burlington, MA, USA)	The cooked gel properties after RF thawing were unaffected; an electrode gap of 16 cm was found to be the best for thawing frozen minced fish.	Yang et al. (2019)

the material, and the frequency ( $f$ , Hz) of the generator (Eq. 8). A dielectric material with a considerable power dissipation capability (a loss material) placed between two plate electrodes (RF heating) interacting with an electromagnetic field is the basis of dielectric heating. To determine the absorbed power density at any point inside the sample, the value of  $E$  must be known, and  $E$  depends on the sample geometry, DPs, and system configuration.

**Heat transfer.** The thawing process is at its most basic a phase change. There are two concomitant phases involved in the complex process of heat conduction in frozen foods, and some energy is absorbed by the latent heat prior to the production of sensible heat. Introducing an apparent specific heat ( $C_{p\text{-app}}$ ) parameter, which accounts for the latent heat of fusion, can simplify matters. In this way, a three-dimensional (3D) heat transfer equation (dependent on the thermophysical properties of the sample) in addition to the internal heat production resulting from dielectric heating can be used to simulate temperature distributions:

$$\rho C_{p\text{-app}} \frac{\partial T}{\partial t} = \nabla(k \nabla T) + P \quad (10)$$

where  $T$  is the temperature (K),  $k$  is the thermal conductivity ( $\text{W m}^{-1} \text{K}^{-1}$ ),  $\rho$  is the density ( $\text{kg m}^{-3}$ ),  $C_{p\text{-app}}$  is expressed in  $\text{J kg}^{-1} \text{K}^{-1}$ , and the internal heat generation is obtained from Eq. 8.

Converting a moving boundary problem into a heat conduction problem with a phase change requires an apparent specific heat term (Succar and Hayakawa 1983). The same governing equation can then be used for both phases, and the moving boundary condition can be implicitly incorporated into the equation (Llave et al. 2015). Fourier's heat equation with a generation term (Eq. 10) can be employed along with the heat generation data to calculate the spatial and transient temperatures. Simultaneous solutions can be obtained using several numerical algorithms and specialized software, described in detail by Awuah, Ramaswamy, and Tang (2014), Huang et al. (2016), and Zhang and Marra (2010). The selection of the appropriate boundary conditions depends of several factors, which include the type and geometry of the sample, the selected solution method, the characteristics of the oven, the assumptions, and others. For details, readers see the article by Chakravorti (2015).

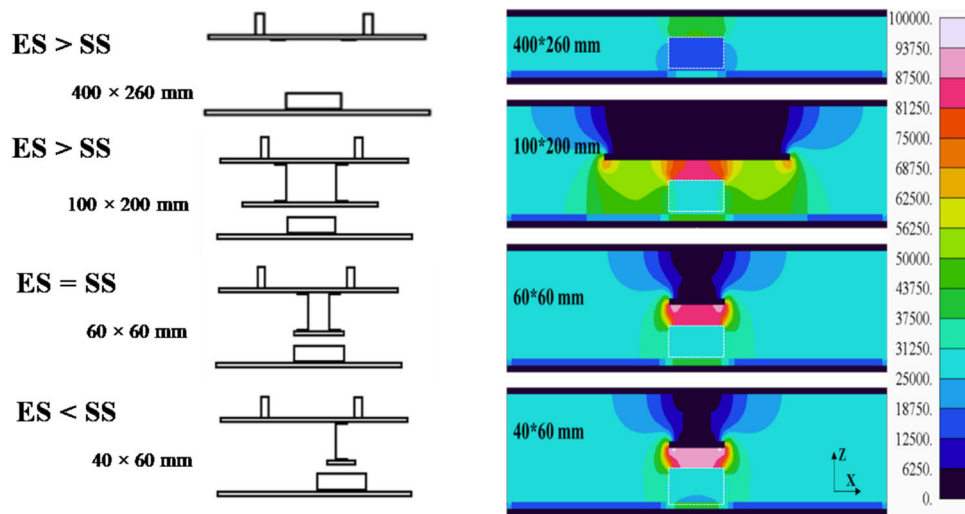


**Figure 10.** (A) Schematic view of the upper electrode and its projections used in the RF system. (B) Simulated electric field distribution after 5 min RF thawing of the whole system using different projection sizes of the upper electrode. [From Llave et al. (2015) with permission of Elsevier].

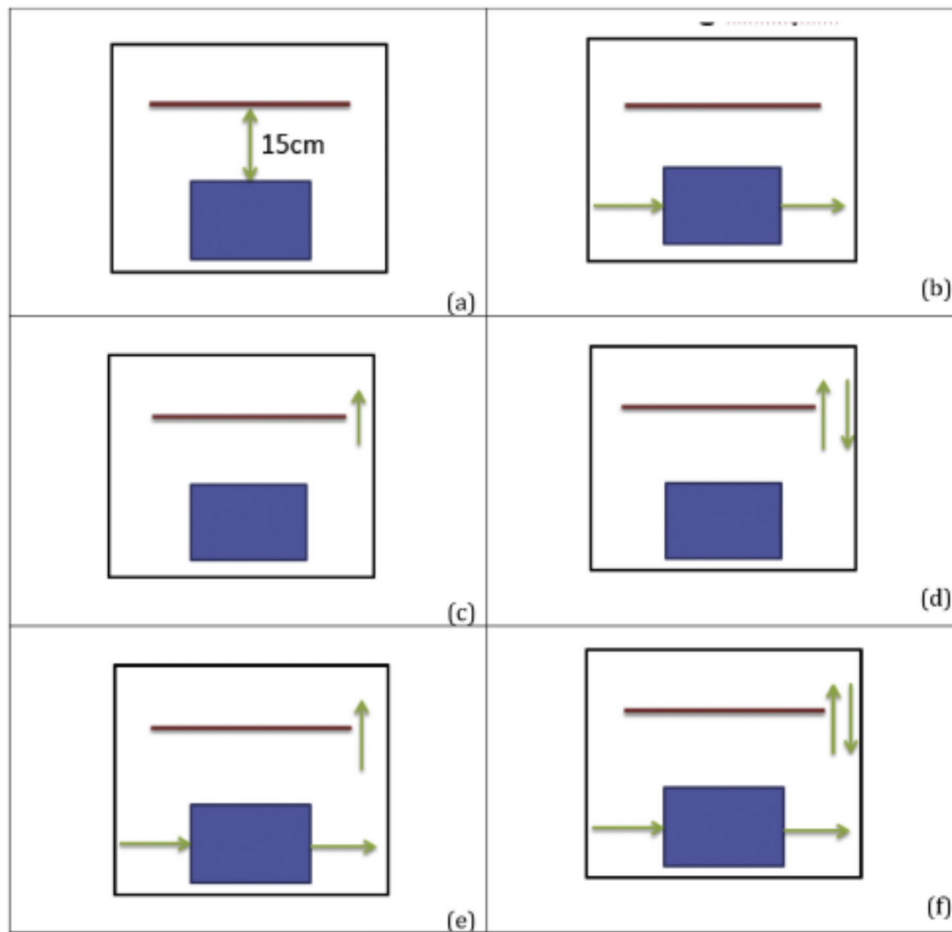


**Figure 11.** Configurations used in the simulations; (a) stable electrode and sample inside the cavity; (b) moving sample ( $1.45 \text{ m h}^{-1}$ ) inside the cavity at constant velocity; (c) moving electrode ( $0.23 \text{ m h}^{-1}$ ) away from the stable sample; (d) moving electrode ( $0.45 \text{ m h}^{-1}$ ) with 1-up and 1-down oscillation through the process; (e) combined effects of electrode moving away after half time ( $0.45 \text{ m h}^{-1}$ ) and sample movement ( $1.45 \text{ m h}^{-1}$ ); (f) moving sample ( $1.45 \text{ m h}^{-1}$ ) with moving electrode with 1-up and 1-down oscillation ( $0.45 \text{ m h}^{-1}$ ). [From Erdogan et al. (2017) with permission of Elsevier].

### Radio frequency defrosting modelling—stationary process

Relevant computer simulation models have been reported in the past focused on the modeling of the RF heating process

to improve heating uniformity (Birla, Wang, and Tang 2008; Chan, Tang, and Younce 2004; Marra et al. 2007; Romano and Marra 2008; Wang et al. 2012). However, in the last five years, novel mathematical approaches have been demonstrated the efficiency in simulate the RF process and



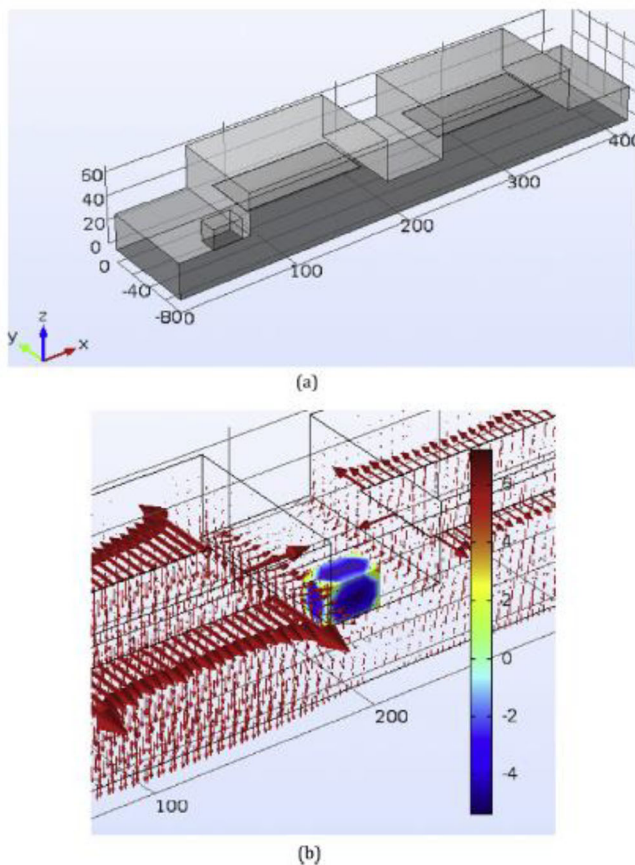


**Figure 12.** (a) Geometrical configuration of the two cavity RF system (the dimensions are given in cm); (b) surface temperature change (°C) of the sample with the electric field ( $\text{V m}^{-1}$ ) within the system. [From Erdogdu et al. (2017) with permission of Elsevier].

showed notable advances in the state of the art in computer simulation of RF defrosting field. As follows, some of them are discussed.

Uyar et al. (2015) developed a computational model to simulate the temperature and electromagnetic field distribution in frozen lean beef during RF thawing for improving the heating uniformity and minimizing runaway heating. Results revealed that a larger block size resulted in a higher absorption of RF power with a shorter thawing time. A similar study was carried out by Llave et al. (2015), who developed a mathematical model for RF defrosting of tuna (*Thunnus maccoyii*). They used a 13.56 MHz parallel-plate RF system to test the simulated results. Based on the mathematical model, the best heating uniformity was found when the size of upper electrode was close to that of the sample's top surface (Figure 10).

### Radio frequency defrosting modelling—continuous process

It has been reported that continuous treatment method is demanded in food industry for the advantages of handling large quantities of products and reducing handling costs. Especially in meat products processing industries, the most common processes like tempering and thawing of frozen products involve larger sized frozen food products to be

processed at the same time and hence require fast and continuous processing methods (Bedane, Chen et al. 2017).

The application of continuous mode (considering a food product moving on conveyor belt) in industrial systems is more desirable than the batch ones because the continuous operation improves the process cost of mass production and quality level of products. In continuous RF processing, the heating uniformity was influenced by physical parameters, such as speed of belt conveyor and consequently, the residence time.

Translational and rotational movement of the food product and electrode vertical movement affect the temperature distribution during RF thawing process due to the changes in the electric field distribution. Considering the significant effect of electric field distribution within an RF system, it would also be possible to suggest optimal process design with a pre-determined electric field distribution. Chen et al. (2017), Bedane, Marra, and Wang (2017), and Palazoglu and Miran (2017) reported that placing the product on a moving conveyor belt might improve temperature uniformity.

Erdogdu et al. (2017) demonstrated various possibilities for movement of the sample and the charged electrode in an RF cavity for power absorption and temperature uniformity during thawing using a computational approach (Figure 11). They developed a mathematical model to consider the movement of the RF electrode and the subsequent effects of temperature and electric field changes. They suggested that two-cavity systems could be a way to overcome the overheating at the corners and edges, where a physical rotation can be carried out in the middle section of the system (Figure 12, showing the geometrical configuration of the two cavity RF system and the surface temperature change of the sample with the electric field ( $\text{V m}^{-1}$ ) within the system). Moreover, the variable electromagnetic potential and moving electrodes were also reported to be applied in the cavities to improve heating uniformity (Erdogdu et al. 2017). Accordingly, these simulated continuous RF thawing protocols showed a potential in industrial use, whereas these RF thawing protocols still need to be confirmed under experimental study.

### Limits and challenges

The RF thawing process still has some negative effects on frozen food quality. However, the disadvantages of large equipment space, the operational inconvenience, large energy consumption, runaway heating, and high cost are slowly being solved. Numerous reports about preventing runaway heating and non-uniformities in RF thawing have been reported in recent years. Strategies for “heating with cold surfaces” and combining thawing technologies have been applied to RF thawing technology to alleviate overheating (Pain and Muller 2014).

Although mathematical modeling and equipping systems with a cooling or heating medium, food movement, and rotation are solutions that are useful to avoid runaway heating in RF process (Hou, Ling, and Wang 2014), more effort



is still needed to find more complete and convenient thawing technologies.

It is desirable to explore the applications of RF thawing/tempering at other frequencies beyond the popular 27.12 MHz. The applicability of different frequency RF to different applications can be studied, such as 40.68 MHz for the small volume rapid heating process, like fruit blanching, and 13.56 MHz for the large long-term heating processing like thawing. Most of the current evaluations are focused on the physical and chemical properties, the structure of proteins, water migration, and lipid oxidation and texture. However, more information about the nutrition and flavor changes after thawing is needed.

## Conclusions

RF heating has been successfully applied for industrial scale thawing/tempering of frozen food processing due to its characteristics of rapid and uniform heating and large penetration depth. RF thawing/tempering can not only provide safe and high-quality defrosted food products but also lead to reduced energy consumption. However, most of the reported applications have been developed using devices at the frequency of 27.12 MHz. It is desirable to explore the applications of RF thawing/tempering at other frequencies for example 13.56 and 40.68 MHz.

Due to the significant change of the DPs within the frozen and thawed stages, a significant temperature non-uniformity was observed for thawing purposes, and tempering has become the objective function as a process aid. To improve thermal uniformity, RF has been reported to be combined with surface cooling (cold air or water/emulsions flow), assisting with sample movement or mixing. The combination of two or more methods can greatly improve the uniformity of heating and the efficiency of treatment. In addition, accurate simulation methods have been reported as feasible design tools in RF systems development and RF treatable foods test. Mathematical modeling approaches were introduced, and rather complex models for moving food products in an industrial scale system were simulated for simultaneous temperature increase, phase change for thawing processes, and changes in the electric field. Thus, the RF heating uniformity can be improved by adjusting the processing parameters of the RF system and properties of food materials leading to better designs of RF equipment. Therefore, it is essential to continue the development of these approaches.

The results explained in this review, provide detailed information to optimize and design processing parameters and to promote further practical applications of RF heating in food thawing/tempering processing industry.

## Declarations of interest

No potential conflict of interest was reported by the authors.

## ORCID

Yvan Llave  <http://orcid.org/0000-0002-8934-9465>

Ferruh Erdogan  <http://orcid.org/0000-0003-3047-4779>

## References

- Awuah, G. B., H. S. Ramaswamy, and J. Tang. 2014. *Radio frequency heating in food processing: Principles and applications*. Boca Raton, FL: CRC Press Taylor and Francis Group.
- Bedane, T. F., O. Altin, B. Erol, F. Marra, and F. Erdogan. 2018. Thawing of frozen food products in a staggered through-field electrode radio frequency system: A case study for frozen chicken breast meat with effects on drip loss and texture. *Innovative Food Science & Emerging Technologies* 50:139–47. doi: [10.1016/j.ifset.2018.09.001](https://doi.org/10.1016/j.ifset.2018.09.001).
- Bedane, T. F., L. Chen, F. Marra, and S. Wang. 2017. Experimental study of radio frequency (RF) thawing of foods with movement on conveyor belt. *Journal of Food Engineering* 201:17–25. doi: [10.1016/j.jfoodeng.2017.01.010](https://doi.org/10.1016/j.jfoodeng.2017.01.010).
- Bedane, T. F., F. Marra, and S. Wang. 2017. Performance comparison between batch and continuous thawing of food products assisted by radio frequency heating. *Chemical Engineering Transactions* 57: 2017–22. doi: [10.3303/CET1757337](https://doi.org/10.3303/CET1757337).
- Bengtsson, N. 1963. Electronic defrosting of meat and fish at 35 and 2450 MHz – A laboratory comparison. *Food Technology* 17 (10): 1309–12.
- Bernard, J. P., J. M. Jacomino, and M. Radoiu. 2015. RF 50  $\Omega$  technology versus variable-frequency RF technology. In *Radio-frequency heating in food processing—Principles and applications*, ed. G. B. Awuah, H. S. Ramaswamy, and J. Tang, Chapter 7, 119–140. Boca Raton, FL: CRC Press Taylor and Francis Group.
- Birla, S. L., S. Wang, and J. Tang. 2008. Computer simulation of radio frequency heating of model fruit immersed in water. *Journal of Food Engineering* 84 (2):270–80. doi: [10.1016/j.jfoodeng.2007.05.020](https://doi.org/10.1016/j.jfoodeng.2007.05.020).
- Boonsumrej, S., S. Chaiwanichsiri, S. Tantratian, T. Suzuki, and R. Takai. 2007. Effects of freezing and thawing on the quality changes of tiger shrimp (*Penaeus monodon*) frozen by air-blast and cryogenic freezing. *Journal of Food Engineering* 80 (1):292–9. doi: [10.1016/j.jfoodeng.2006.04.059](https://doi.org/10.1016/j.jfoodeng.2006.04.059).
- Boreddy, S. R., and J. Subbiah. 2016. Temperature and moisture dependent dielectric properties of egg white powder. *Journal of Food Engineering* 168:60–7. doi: [10.1016/j.jfoodeng.2015.07.023](https://doi.org/10.1016/j.jfoodeng.2015.07.023).
- Cai, L., M. Cao, A. Cao, J. Regenstein, J. Li, and R. Guan. 2018. Ultrasound or microwave vacuum thawing of red seabream (*Pagrus major*) fillets. *Ultrasonics Sonochemistry* 47:122–32. doi: [10.1016/j.ultrsonch.2018.05.001](https://doi.org/10.1016/j.ultrsonch.2018.05.001).
- Cai, L., M. Cao, J. Regenstein, and A. Cao. 2019. Recent advances in food thawing technologies. *Comprehensive Reviews in Food Science and Food Safety* 18 (4):953–70. doi: [10.1111/1541-4337.12458](https://doi.org/10.1111/1541-4337.12458).
- Cathcart, W., and J. J. Parker. 1946. Defrosting frozen foods by high-frequency heat. *Food Research* 11 (4):341–4. doi: [10.1111/j.1365-2621.1946.tb16359.x](https://doi.org/10.1111/j.1365-2621.1946.tb16359.x).
- Chakravorti, S. 2015. *Electric field analysis (Chapter 6)*. Boca Raton, FL: CRC Press Taylor and Francis Group.
- Chamchong, M., and A. K. Datta. 1999. Thawing of foods in a microwave oven: I. Effect of power levels and power cycling. *Journal of Microwave Power and Electromagnetic Energy* 34 (1):9–21. doi: [10.1080/08327823.1999.11688384](https://doi.org/10.1080/08327823.1999.11688384).
- Chan, T. V., J. Tang, and F. Younce. 2004. 3-Dimensional numerical modeling of an industrial radio frequency heating system using finite elements. *Journal of Microwave Power and Electromagnetic Energy* 39 (2):87–105. doi: [10.1080/08327823.2004.11688511](https://doi.org/10.1080/08327823.2004.11688511).
- Chen, J., J. Tang, and F. Liu. 2008. Simulation model for moving food packages in microwave heating processes using conformal FDTD method. *Journal of Food Engineering* 88 (3):294–305. doi: [10.1016/j.jfoodeng.2008.02.020](https://doi.org/10.1016/j.jfoodeng.2008.02.020).
- Chen, Q., D. M. Fan, H. W. Cao, J. L. Huang, J. X. Zhao, B. W. Yan, W.-g. Zhou, W.-h. Zhang, and H. Zhang. 2017. Study on thawing

- effect of radio frequency on frozen minced fish. *Food Research & Development* 38 (22):90–6. doi: [10.3969/j.issn.1005-6521.2017.22.019](https://doi.org/10.3969/j.issn.1005-6521.2017.22.019).
- Chen, Y., J. He, F. Li, J. Tang, and Y. Jiao. 2021. Model food development for tuna (*Thunnus obesus*) in radio frequency and microwave tempering using grass carp mince. *Journal of Food Engineering* 292: 110267. doi: [10.1016/j.jfoodeng.2020.110267](https://doi.org/10.1016/j.jfoodeng.2020.110267).
- Choi, E. J., H. W. Park, H. S. Yang, J. S. Kim, and H. H. Chun. 2017. Effects of 27.12 MHz radio frequency on the rapid and uniform tempering of cylindrical frozen pork loin (*Longissimus thoracis et lumborum*). *Korean Journal for Food Science of Animal Resources* 37 (4): 518–28. doi: [10.5851/kosfa.2017.37.4.518](https://doi.org/10.5851/kosfa.2017.37.4.518).
- Choi, W., S. H. Lee, C. T. Kim, and S. Jun. 2015. A finite element method based flow and heat transfer model of continuous flow microwave and ohmic combination heating of particulate foods. *Journal of Food Engineering* 149:159–70. doi: [10.1016/j.jfoodeng.2014.10.016](https://doi.org/10.1016/j.jfoodeng.2014.10.016).
- Curet, S., O. Rouaud, and L. Boillereaux. 2014. Estimation of dielectric properties of food materials during microwave tempering and heating. *Food and Bioprocess Technology* 7 (2):371–84. doi: [10.1007/s11947-013-1061-4](https://doi.org/10.1007/s11947-013-1061-4).
- Datta, A. K., G. Sumnu, and G. S. V. Raghavan. 2014. Dielectric properties of foods. In *Engineering properties of foods*, ed. M. A. Rao, S. S. H. Rizvi, A. K. Datta, and J. Ahmed, Chapter 14. Boca Raton, FL: CRC Press Taylor and Francis Group.
- Erdogdu, F., O. Altin, F. Marra, and T. F. Bedane. 2017. A computational study to design process conditions in industrial radio-frequency tempering/thawing process. *Journal of Food Engineering* 213: 99–112. doi: [10.1016/j.jfoodeng.2017.05.003](https://doi.org/10.1016/j.jfoodeng.2017.05.003).
- Farag, K. W., E. Duggan, D. J. Morgan, D. A. Cronin, and J. G. Lyng. 2009. A comparison of conventional and radio frequency defrosting of lean beef meats: Effects on water binding characteristics. *Meat Science* 83 (2):278–84. doi: [10.1016/j.meatsci.2009.05.010](https://doi.org/10.1016/j.meatsci.2009.05.010).
- Farag, K. W., J. G. Lyng, D. J. Morgan, and D. A. Cronin. 2008. A comparison of conventional and radio frequency tempering of beef meats: Effects on product temperature distribution. *Meat Science* 80 (2):488–95. doi: [10.1016/j.meatsci.2008.01.015](https://doi.org/10.1016/j.meatsci.2008.01.015).
- Farag, K. W., J. G. Lyng, D. J. Morgan, and D. A. Cronin. 2011. A comparison of conventional and radio frequency tempering of beef meats: Effects on product temperature distribution. *Food and Bioprocess Technology* 4 (7):1128–36. doi: [10.1007/s11947-009-0205-z](https://doi.org/10.1007/s11947-009-0205-z).
- FDA Food Code. 2013. *U.S. Department of Health and Human Sciences, public health service*. Vol. 20740, 89–90. College Park, MD: Food and Drug Administration.
- Ferrari, J. R. S., J. Katrib, P. Palade, A. R. Batchelor, C. Dodds, and S. W. Kingman. 2016. A tool for predicting heating uniformity in industrial radio frequency processing. *Food and Bioprocess Technology* 9 (11):1865–73. doi: [10.1007/s11947-016-1762-6](https://doi.org/10.1007/s11947-016-1762-6).
- Fiore, A., R. Di Monaco, S. Cavella, A. Visconti, O. Karneili, S. Bernhardt, and V. Fogliano. 2013. Chemical profile and sensory properties of different foods cooked by a new radiofrequency oven. *Food Chemistry* 139 (1–4):515–20. doi: [10.1016/j.foodchem.2013.01.028](https://doi.org/10.1016/j.foodchem.2013.01.028).
- Gambuteanu, C., and P. Alexe. 2015. Comparison of thawing assisted by low-intensity ultrasound on technological properties of pork *longissimus dorsi* muscle. *Journal of Food Science and Technology* 52 (4):2130–8. doi: [10.1007/s13197-013-1204-7](https://doi.org/10.1007/s13197-013-1204-7).
- Gökoğlu, N., and P. Yerlikaya. 2015. *Seafood chilling, refrigeration and freezing: Science and technology*. West Sussex, UK: John Wiley & Sons.
- Guo, C., A. S. Mujumdar, and M. Zhang. 2019. New development in radio frequency heating for fresh food processing: A review. *Food Engineering Reviews* 11 (1):29–43. doi: [10.1007/s12393-018-9184-z](https://doi.org/10.1007/s12393-018-9184-z).
- Guan, D., M. Cheng, Y. Wang, and J. Tang. 2004. Dielectric properties of mashed potatoes relevant to microwave and radio-frequency pasteurization and sterilization processes. *Journal of Food Science* 69 (1):FEP30–FEP37. doi: [10.1111/j.1365-2621.2004.tb17864.x](https://doi.org/10.1111/j.1365-2621.2004.tb17864.x).
- Hansen, J. D., S. R. Drake, M. A. Watkins, M. L. Heidt, P. A. Anderson, and J. Tang. 2006. Radio frequency pulse application for heating uniformity in postharvest codling moth (*Lepidoptera tortricidae*) control of fresh apples (*Malus domestica borkh.*). *Journal of Food Quality* 29 (5):492–504. doi: [10.1111/j.1745-4557.2006.00089.x](https://doi.org/10.1111/j.1745-4557.2006.00089.x).
- Hou, L., B. Ling, and S. Wang. 2014. Development of thermal treatment protocol for disinfecting chestnuts using radio frequency energy. *Postharvest Biology and Technology* 98:65–71. doi: [10.1016/j.postharvbio.2014.07.007](https://doi.org/10.1016/j.postharvbio.2014.07.007).
- Huang, Z., F. Marra, and S. Wang. 2016. A novel strategy for improving radio frequency heating uniformity of dry food products using computational modeling. *Innovative Food Science & Emerging Technologies* 34:100–11. doi: [10.1016/j.ifset.2016.01.005](https://doi.org/10.1016/j.ifset.2016.01.005).
- Icier, F., and T. Baizal. 2004. Dielectrical properties of food materials—2: Measurement techniques. *Critical Reviews in Food Science and Nutrition* 44 (6):473–8. doi: [10.1080/10408690490892361](https://doi.org/10.1080/10408690490892361).
- Izadifar, M., and O. D. Baik. 2008. Dielectric properties of a packed bed of the rhizome of *P. peltatum* with an ethanol/water solution for radio frequency-assisted extraction of podophyllotoxin. *Biosystems Engineering* 100 (3):376–88. doi: [10.1016/j.biosystemseng.2008.04.007](https://doi.org/10.1016/j.biosystemseng.2008.04.007).
- Jeong, S. G., and D. H. Kang. 2014. Influence of moisture content on inactivation of *Escherichia coli* O157:H7 and *Salmonella enterica* serovar Typhimurium in powdered red and black pepper spices by radio-frequency heating. *International Journal of Food Microbiology* 176:15–22. doi: [10.1016/j.ijfoodmicro.2014.01.011](https://doi.org/10.1016/j.ijfoodmicro.2014.01.011).
- Jia, G. L., X. L. He, S. Nirasawa, E. Tatsumi, H. J. Liu, and H. J. Liu. 2017. Effect of high-voltage electrostatic field on the freezing behavior and quality of pork tenderloin. *Journal of Food Engineering* 204: 18–26. doi: [10.1016/j.jfoodeng.2017.01.020](https://doi.org/10.1016/j.jfoodeng.2017.01.020).
- Jiao, Y., D. Luan, and J. Tang. 2014. Principles of radio-frequency and microwave heating. In *Radio-frequency heating in food processing: Principles and applications*, ed. G. B. Awuah, H. S. Ramaswamy, and J. Tang, Chapter 1. Boca Raton, FL: Taylor & Francis Group.
- Jiao, Y., J. Tang, S. Wang, and T. Koral. 2014. Influence of dielectric properties on the heating rate in free-running oscillator radio frequency systems. *Journal of Food Engineering* 120:197–203. doi: [10.1016/j.jfoodeng.2013.07.032](https://doi.org/10.1016/j.jfoodeng.2013.07.032).
- Jiao, Y., J. Tang, Y. Wang, and T. L. Koral. 2018. Radio-frequency applications for food processing and safety. *Annual Review of Food Science and Technology* 9:105–27. doi: [10.1146/annurev-food-041715-033038](https://doi.org/10.1146/annurev-food-041715-033038).
- Karthikeyan, J. S., M. K. Desai, D. Salvi, R. Bruins, and M. K. Karwe. 2015. Effect of temperature abuse on frozen army rations. Part I: Developing a heat transfer numerical model based on thermos-physical properties. *Food Research International* 76:595–604. doi: [10.1016/j.foodres.2015.07.007](https://doi.org/10.1016/j.foodres.2015.07.007).
- Kim, J., J. W. Park, S. Park, D. S. Choi, S. R. Choi, Y. H. Kim, S. J. Lee, C. W. Park, G. J. Han, and B.-K. Cho. 2016. Study of radio frequency thawing for cylindrical pork sirloin. *Journal of Biosystems Engineering* 41 (2):108–15. doi: [10.5307/JBE.2016.41.2.108](https://doi.org/10.5307/JBE.2016.41.2.108).
- Knoerzer, K., M. Regier, and H. Schubert. 2008. A computational model for calculating temperature distributions in microwave food applications. *Innovative Food Science & Emerging Technologies* 9 (3): 374–84. doi: [10.1016/j.ifset.2007.10.007](https://doi.org/10.1016/j.ifset.2007.10.007).
- Li, B., and D.-W. Sun. 2002. Novel methods for rapid freezing and thawing of foods—A review. *Journal of Food Engineering* 54 (3): 175–82. doi: [10.1016/S0260-8774\(01\)00209-6](https://doi.org/10.1016/S0260-8774(01)00209-6).
- Li, D., H. Zhao, A. I. Muhamma, L. Song, M. Guo, and D. Liu. 2020. The comparison of ultrasound-assisted thawing, air thawing and water immersion thawing on the quality of slow/fast freezing big-head carp (*Aristichthys nobilis*) fillets. *Food Chemistry* 320:126614. doi: [10.1016/j.foodchem.2020.126614](https://doi.org/10.1016/j.foodchem.2020.126614).
- Li, Y., F. Li, J. Tang, R. Zhang, Y. Wang, T. Koral, and Y. Jiao. 2018. Radio frequency tempering uniformity investigation of frozen beef with various shapes and sizes. *Innovative Food Science & Emerging Technologies* 48:42–55. doi: [10.1016/j.ifset.2018.05.008](https://doi.org/10.1016/j.ifset.2018.05.008).
- Liu, C., and N. Sakai. 1999. Dielectric properties of tuna at 2450 MHz and 915 MHz as a function of temperature. *Nippon Shokuhin Kagaku Kogaku Kaishi* 46 (10):652–6. (in Japanese). doi: [10.3136/nskkk.46.652](https://doi.org/10.3136/nskkk.46.652).

- Liu, L., Y. Llave, Y. Jin, D.-Y. Zheng, M. Fukuoka, and N. Sakai. 2017. Electrical conductivity and ohmic thawing of frozen tuna at high frequencies. *Journal of Food Engineering* 197:68–77. doi: [10.1016/j.jfoodeng.2016.11.002](https://doi.org/10.1016/j.jfoodeng.2016.11.002).
- Llave, Y., D. Kambayashi, M. Fukuoka, and N. Sakai. 2020. Power absorption analysis of two-component materials during microwave thawing and heating: Experimental and computer simulation. *Innovative Food Science & Emerging Technologies* 66:102479. doi: [10.1016/j.ifset.2020.102479](https://doi.org/10.1016/j.ifset.2020.102479).
- Llave, Y., S. Liu, M. Fukuoka, and N. Sakai. 2015. Computer simulation of radio frequency defrosting of frozen foods. *Journal of Food Engineering* 152:32–42. doi: [10.1016/j.jfoodeng.2014.11.020](https://doi.org/10.1016/j.jfoodeng.2014.11.020).
- Llave, Y., K. Mori, D. Kambayashi, M. Fukuoka, and N. Sakai. 2016. Dielectric properties and model food application of tylose water pastes during microwave thawing and heating. *Journal of Food Engineering* 178:20–30. doi: [10.1016/j.jfoodeng.2016.01.003](https://doi.org/10.1016/j.jfoodeng.2016.01.003).
- Llave, Y., and N. Sakai. 2018. Dielectric defrosting of frozen foods. In *Handbook of food bioengineering (Multi volume set—Volume XVIII: Food processing for increased quality and consumption)*, ed. A. M. Grumezescu and A. M. Holban, Chapter 13. London, UK: Elsevier.
- Llave, Y., Y. Terada, M. Fukuoka, and N. Sakai. 2014. Dielectric properties of frozen tuna and analysis of defrosting using a radio-frequency system at low frequencies. *Journal of Food Engineering* 139: 1–9. doi: [10.1016/j.jfoodeng.2014.04.012](https://doi.org/10.1016/j.jfoodeng.2014.04.012).
- Maloney, N., and M. Harrison. 2016. Advanced heating technologies for food processing. In *Innovation and future trends in food manufacturing and supply chain technologies*, ed. C. Leadley, Chapter 8. Campden BRI, UK: Elsevier. doi: [10.1016/C2014-0-01383-4](https://doi.org/10.1016/C2014-0-01383-4).
- Margulies, S. 1984. Force on a dielectric slab inserted into a parallel-plate capacitor. *American Journal of Physics* 52 (6):515–8. doi: [10.1119/1.13861](https://doi.org/10.1119/1.13861).
- Marra, F., J. Lyng, V. Romano, and B. McKenna. 2007. Radio-frequency heating of foodstuff: Solution and validation of a mathematical model. *Journal of Food Engineering* 79 (3):998–1006. doi: [10.1016/j.jfoodeng.2006.03.031](https://doi.org/10.1016/j.jfoodeng.2006.03.031).
- Metaxas, A. C. 1996. *Foundations of electroheat: A unified approach*. New York: Wiley.
- Mitchell, L. 2016. *The wave of the future*. Retrieved January 6, 2016, from [https://www.radiofrequency.com/pdfs/rf\\_pasteurization.pdf](https://www.radiofrequency.com/pdfs/rf_pasteurization.pdf)
- Ozturk, S., F. B. Kong, S. Trabelsi, and R. K. Singh. 2016. Dielectric properties of dried vegetable powders and their temperature profile during radio frequency heating. *Journal of Food Engineering* 169: 91–100. doi: [10.1016/j.jfoodeng.2015.08.008](https://doi.org/10.1016/j.jfoodeng.2015.08.008).
- Pain, J. P., and F. L. Muller. 2014. Modeling basics as applied to ohmic heating of liquid and wall cooling. In *Ohmic heating in food processing*, ed. H. S. Ramaswamy, M. Marcotte, S. Sastry, and K. Abdelrahim, Chapter 15. Boca Raton, FL: CRC Press, Taylor & Francis Group.
- Palazoglu, T. K., and W. Miran. 2017. Experimental comparison of microwave and radio frequency tempering of frozen block of shrimp. *Innovative Food Science & Emerging Technologies* 41: 292–300. doi: [10.1016/j.ifset.2017.04.005](https://doi.org/10.1016/j.ifset.2017.04.005).
- Pereira, R. N., and A. A. Vicente. 2010. Environmental impact of novel thermal and non-thermal technologies in food processing. *Food Research International* 43 (7):1936–43. doi: [10.1016/j.foodres.2009.09.013](https://doi.org/10.1016/j.foodres.2009.09.013).
- Piyasena, P., C. Dussault, T. Koutchma, H. S. Ramaswamy, and G. B. Awuah. 2003. Radio frequency heating of foods: Principles, applications and related properties—a review. *Critical Reviews in Food Science and Nutrition* 43 (6):587–606. doi: [10.1080/10408690390251129](https://doi.org/10.1080/10408690390251129).
- Rattanadecho, P. 2004. Theoretical and experimental investigation of microwave thawing of frozen layer using a microwave oven (effects of layered configurations and layer thickness). *International Journal of Heat and Mass Transfer* 47 (5):937–45. doi: [10.1016/j.ijheatmasstransfer.2003.08.019](https://doi.org/10.1016/j.ijheatmasstransfer.2003.08.019).
- Romano, V., and F. Marra. 2008. A numerical analysis of radio frequency heating of regular shaped foodstuff. *Journal of Food Engineering* 84 (3):449–57. doi: [10.1016/j.jfoodeng.2007.06.006](https://doi.org/10.1016/j.jfoodeng.2007.06.006).
- Rouille, J., A. Lebail, H. S. Ramaswamy, and L. Leclerc. 2002. High pressure thawing of fish and shellfish. *Journal of Food Engineering* 53 (1):83–8. doi: [10.1016/S0260-8774\(01\)00143-1](https://doi.org/10.1016/S0260-8774(01)00143-1).
- Sato, M., T. Yamaguchi, and T. Nakano. 2016. Method of thawing frozen food. US Patent No. 0192-0667. Washington, DC: US Patent and Trademark Office.
- Singh, R. P., F. Erdogdu, and J. Mannapperuma. 2002. *Industrial-Scale Food Freezing Simulation Software (V.3.0)*. Bethesda, MD: WFLO—World Food Logistics Organization.
- Succar, J., and K. Hayakawa. 1983. Empirical formulas for predicting thermal physical properties of food at freezing or defrosting temperature. *LWT-Food Science and Technology* 16:326–31.
- Swamy, G. J., and K. Muthukumarappan. 2021. Microwave and radio-frequency processing of plant-related food products. In *Innovative food processing technologies, A comprehensive review*, ed. K. Knoerzer and K. Muthukumarappan, Chapter 8. London, UK: Elsevier.
- Taher, B. J., and M. M. Farid. 2001. Cyclic microwave thawing of frozen meat: Experimental and theoretical investigation. *Chemical Engineering and Processing: Process Intensification* 40 (4):379–89. doi: [10.1016/S0255-2701\(01\)00118-0](https://doi.org/10.1016/S0255-2701(01)00118-0).
- Trabelsi, S. 2015. Variation of the dielectric properties of chicken meat with frequency and temperature. *Journal of Food Measurement and Characterization* 9 (3):299–304. doi: [10.1007/s11694-015-9235-6](https://doi.org/10.1007/s11694-015-9235-6).
- Uan, D. G., M. Cheng, Y. Wang, and J. Tang. 2004. Dielectric properties of mashed potatoes relevant to microwave and radio-frequency pasteurization and sterilization processes. *Journal of Food Science* 69 (1):FEP30–37. doi: [10.1111/j.1365-2621.2004.tb17864.x](https://doi.org/10.1111/j.1365-2621.2004.tb17864.x).
- Uyar, R., T. F. Bedane, F. Erdogdu, T. K. Palazoglu, K. W. Farag, and F. Marra. 2015. Radio-frequency thawing of food products—A computational study. *Journal of Food Engineering* 146:163–71. doi: [10.1016/j.jfoodeng.2014.08.018](https://doi.org/10.1016/j.jfoodeng.2014.08.018).
- Uyar, R., F. Erdogdu, and F. Marra. 2014. Effect of load volume on power absorption and temperature evolution during radio-frequency heating of meat cubes: A computational study. *Food and Bioprocess Technology* 92 (3):243–51. doi: [10.1016/j.fbp.2013.12.005](https://doi.org/10.1016/j.fbp.2013.12.005).
- Von Hippel, A. R. 1954. *Dielectric and waves*. New York: Wiley.
- Wang, B., X. Du, B. Kong, Q. Liu, F. Li, N. Pan, X. Xia, and D. Zhang. 2020. Effect of ultrasound thawing, vacuum thawing, and microwave thawing on gelling properties of protein from porcine *logissimus dorsi*. *Ultrasonics Sonochemistry* 64:104860. doi: [10.1016/j.ultsonch.2019.104860](https://doi.org/10.1016/j.ultsonch.2019.104860).
- Wang, J., K. Luechapattaporn, Y. Wang, and J. Tang. 2012. Radio-frequency heating of heterogeneous food-meat lasagna. *Journal of Food Engineering* 108 (1):183–93. doi: [10.1016/j.jfoodeng.2011.05.031](https://doi.org/10.1016/j.jfoodeng.2011.05.031).
- Wang, S., J. Tang, J. A. Johnson, E. Mitcham, J. D. Hansen, G. Hallman, S. R. Drake, and Y. Wang. 2003. Dielectric properties of fruits and insect pest as related to radio frequency and microwave treatments. *Biosystems Engineering* 85 (2):201–12. doi: [10.1016/S1537-5110\(03\)00042-4](https://doi.org/10.1016/S1537-5110(03)00042-4).
- Wang, Y. Y., Y. R. Li, S. J. Wang, Z. Li, M. X. Gao, and J. M. Tang. 2011. Review of dielectric drying of fruits and agricultural products. *International Journal of Agricultural and Biological Engineering* 4: 1–19. doi: [10.3965/j.issn.1934-6344.2011.01.001-019](https://doi.org/10.3965/j.issn.1934-6344.2011.01.001-019).
- Yang, H., Q. Chen, H. Cao, D. Fan, J. Huang, J. Zhao, B. Yan, W. Zhou, W. Zhang, and H. Zhang. 2019. Radiofrequency thawing of frozen minced fish based on the dielectric response mechanism. *Innovative Food Science & Emerging Technologies* 52:80–8. doi: [10.1016/j.ifset.2018.10.013](https://doi.org/10.1016/j.ifset.2018.10.013).
- Yu, L. H., E. S. Lee, J. Y. Jeong, H. D. Paik, J. H. Choi, and C. J. Kim. 2005. Effects of thawing temperature on the physicochemical properties of pre-rigor frozen chicken breast and leg muscles. *Meat Science* 71 (2):375–82. doi: [10.1016/j.meatsci.2005.04.020](https://doi.org/10.1016/j.meatsci.2005.04.020).
- Zhang, L., J. G. Lyng, and N. P. Brunton. 2004. Effect of radio frequency cooking on the texture, colour and sensory properties of a large diameter comminuted meat product. *Meat Science* 68 (2): 257–68. doi: [10.1016/j.meatsci.2004.03.011](https://doi.org/10.1016/j.meatsci.2004.03.011).
- Zhang, L., and F. Marra. 2010. Radio frequency heating of foods. In *Mathematical modeling of food processing*, ed. M. M. Farid, 691–706. Boca Raton, FL: CRC Press Taylor and Francis Group.



- Zhang, M., H. Jiang, and R. Lim. 2010. Recent developments in microwave-assisted drying of vegetables, fruits, and aquatic products—drying kinetics and quality considerations. *Drying Technology* 28 (11): 1307–16. – doi: [10.1080/07373937.2010.524591](https://doi.org/10.1080/07373937.2010.524591).
- Zhang, R., F. Li, J. Tang, T. Koral, and Y. Jiao. 2020. Improved accuracy of radio frequency (RF) heating simulations using 3D scanning techniques for irregular-shape food. *LWT* 121:108951. doi: [10.1016/j.lwt.2019.108951](https://doi.org/10.1016/j.lwt.2019.108951).
- Zhang, S., L. Y. Zhou, B. Ling, and S. J. Wang. 2016. Dielectric properties of peanut kernels associated with microwave and radio frequency drying. *Biosystems Engineering* 145:108–17. doi: [10.1016/j.biosystemseng.2016.03.002](https://doi.org/10.1016/j.biosystemseng.2016.03.002).
- Zhao, Y., B. Flugstad, E. Kolbe, J. W. Park, and J. H. Wells. 2000. Using capacitive (radio frequency) dielectric heating in food processing and preservation—A review. *Journal of Food Process Engineering* 23 (1):25–55. doi: [10.1111/j.1745-4530.2000.tb00502.x](https://doi.org/10.1111/j.1745-4530.2000.tb00502.x).
- Zhu, S. M., G. M. Su, J. S. He, H. S. Ramaswamy, A. L. Bail, and Y. Yu. 2014. Water phase transition under pressure and its application in high pressure thawing of agar gel and fish. *Journal of Food Engineering* 125:1–6. doi: [10.1016/j.jfoodeng.2013.10.016](https://doi.org/10.1016/j.jfoodeng.2013.10.016).
- Zhu, X. H., W. C. Guo, and Y. P. Jia. 2014. Temperature-dependent dielectric properties of raw cow's and goat's milk from 10 to 4,500 MHz relevant to radio-frequency and microwave pasteurization. *Food and Bioprocess Technology* 7 (6):1830–9. doi: [10.1007/s11947-014-1255-4](https://doi.org/10.1007/s11947-014-1255-4).
- Zhu, Y., F. Li, J. Tang, T. T. Wang, and Y. Jiao. 2019. Effects of radio frequency, air and water tempering, and different end-point tempering temperatures on pork quality. *Journal of Food Process Engineering* 42 (4). doi: [10.1111/jfpe.13026](https://doi.org/10.1111/jfpe.13026).